Electronic Supporting Information (ESI)

A novel pyrazolium ionic liquid used for CO_2 cycloaddition

Jun-Fei Li†[a], Xiao-Hui Guan†[a], Hui-Jun Feng,[a] Dai-Mei Zhou[a], Qiao-Yun Liu*[a], Wen-Yao Zhang [a], Cai-Hong Guo*[a], Jun-Hua Bai[a] and Jun-Wen Wang*[a]

[a]Key Laboratory of Magnetic Molecules and Magnetic Information Materials of Ministry of Education & School of Chemistry and Materials Science of Shanxi Normal University, TaiYuan 030032, China.

*E-mail: wangjunwen2013@163.com

Experimental section

1.1. Materials and Methods.

All starting chemicals and reagents were purchased from commercial suppliers and used as received, unless otherwise mentioned. Spectroscopic measurements were conducted under ambient conditions using dry solvents. The FT-IR spectra were recorded using KBr pellets in the range of 4000–400 cm^{-1} on a Varian 660-IR spectrometer. Nuclear magnetic resonance (NMR) spectra were obtained on a Bruker Avance III HD (600 MHz) spectrometer. The chemical shifts are expressed in parts per million (ppm) with TMS as internal standard. Thermogravimetric analysis (TGA) measurements were carried out on a NETZSCH DSC 200F3 instrument equipped with an automatically programmed temperature controller. The TGA curves were measured in an air atmosphere by heating the samples from 30 °C to 800 °C at a rate of 10 °C min^{-1}. Scanning electron microscopy (SEM) images were recorded using a JEOL JSM-7500F instrument under an accelerating voltage of 20–30 kV. X-ray photoelectron spectroscopy (XPS) data were obtained using a Thermo K-Alpha^{+}scientific electron spectrometer using Al Kα radiation. The N_2 isotherm measurements were carried out at 77 K in a liquid nitrogen bath. The samples were heated to 120 °C and kept at this temperature for at least 12 hours under vacuum for activation. The dry samples were thereafter loaded into sample tubes and activated under high vacuum (less than 10^{-5} Torr) at 200 °C. The apparent surface areas were calculated from nitrogen adsorption data by multipoint BET analysis. The apparent micropore distributions were calculated from nitrogen adsorption data by the NLDFT method. Elemental analyses (C, H, N) were performed on a Perkin-Elmer 240 elemental analyzer.

1.2. Synthesis of 3,5-dimethyl-1,2-bis(phenylmethyl)-1H-Pyrazolium, bromide ([Bn_2DMPz]Br)

After mixing 5 ml of dimethyl sulfoxide and 5.60 g (0.10 mol) of potassium hydroxide in a 50 ml round bottom flask and stirring for 20 minutes, the mixture was added with 4.81 g (0.05 mol) of 3,5-dimethyl-1H-pyrazole at room temperature and stirred for 10 minutes. Subsequently, 7.56 g (0.06 mol) of benzyl chloride was slowly added and the mixture was stirred at room temperature for 3 hours. Upon completion

of the reaction, the product obtained was 9.10 g of yellow liquid 1-benzyl-3,5-dimethyl-1H-pyrazole, with a yield of 97.8%. Then, into a 50 mL round-bottom flask, introduce 5.59 g (0.03 mol) of 1-benzyl-3,5-dimethyl-1H-pyrazole, and carefully add 3.56 ml (0.03 mol) of benzyl bromide using a pressure-equalizing funnel. The reaction occurs at 120 °C without solvent for 2 hours, resulting in the precipitation of a solid. The mixture is subsequently filtered while hot and washed multiple times with ethyl acetate, yielding 3,5-dimethyl-1,2-bis(phenylmethyl)-1H-Pyrazolium, bromide as a white solid of 10.39 g with a 97% yield. ^{1}H NMR (600 MHz, $CDCl_3$, ppm) δ=7.18–7.15 (m, 6H), 6.90 (s, 4H), 6.62 (s, 1H), 5.92 (s, 4H), 2.55 (s, 6H).^{13}C NMR (151 MHz, $CDCl_3$, ppm) δ=147.73, 131.58, 129.30, 128.76, 126.12, 109.20, 51.59, 12.90. Anal. calcd for $C_{19}H_{21}BrN_2$: C, 63.87; H, 5.93; N, 7.84. Found: C, 63.82; H, 5.97; N, 7.72. HR-MS (QTOF) calcd. for $[C_{19}H_{21}N_2+H^+]^+$ m/z: 278.39, found: 277.17. ^{1}H and ^{13}C NMR spectra are showed in Fig. S1 and S2.

1.3. Synthesis of 3,5-dimethyl-1,2-bis[(4-bromophenyl)methyl]-1H-Pyrazolium, bromide ([Bn_2DMBr_2Pz]Br)

After mixing 5 ml of dimethyl sulfoxide and 5.60 g (0.10 mol) of potassium hydroxide in a 50 ml round bottom flask and stirring for 20 minutes, the mixture was added with 4.81 g (0.05 mol) of 3,5-dimethyl-1H-pyrazole at room temperature and stirred for 10 minutes. Subsequently, 12.30 g (0.06 mol) of 4-bromobenzyl chloride was slowly added and the mixture was stirred at room temperature for 3 hours. Upon completion of the reaction, the product obtained was 12.91 g of yellow liquid 1-(4-bromo-benzyl)-3,5-dimethyl-1H-pyrazole, with a yield of 97.4%. Into a 50 mL round-bottom flask, introduce 7.95 g (0.03 mol) of 1-(4-bromo-benzyl)-3,5-dimethyl-1H-pyrazole, and then carefully add 7.49 g (0.03 mol) of 4-bromobenzyl bromide using a pressure-equalizing funnel. The reaction occurs at 120 °C without solvent for 2 hours, resulting in the precipitation of a solid. The mixture is subsequently filtered while hot and washed multiple times with ethyl acetate, yielding 3,5-dimethyl-1,2-bis[(4-bromophenyl)methyl]-1H-Pyrazolium, bromide as a white solid of 14.52 g with a 94.0% yield. ^{1}H NMR (600 MHz, DMSO) δ =7.43 (d, J = 8.4 Hz, 2H), 6.89 (d, J = 8.4 Hz, 2H), 6.88 (s, 1H), 5.71 (s, 2H), 2.48 (s, 3H). ^{13}C NMR (151 MHz, DMSO) δ =148.75,

132.87, 132.13, 128.89, 121.89, 109.38, 49.40, 12.30. Anal. calcd for $C_{19}H_{19}Br_3N_2$: C, 44.30; H, 3.72; N, 5.44. Found: C, 44.38; H, 3.65; N, 5.51. HR-MS (QTOF) calcd. for $[C_{19}H_{19}Br_2N_2+H^+]^+$ m/z: 436.18, found: 434.98. ^1H and ^{13}C NMR spectra are showed in Fig. S5 and S6.

1.4. Synthesis of DDP

A mixture of 3,5-dimethyl-1,2-bis[(4-bromophenyl)methyl]-1H-Pyrazolium, bromide (0.3 mmol, 154.5 mg) and 1,3,5-phenyltriboronic acid (0.2 mmol, 91.2 mg) using dioxane /water (3.0/1.0 mL, v/v 3:1) as the solvent with K_2CO_3 (1.0 mmol, 138.2 mg) and $Pd(PPh_3)_4$ (0.02 mmol, 23.1 mg) was stirred at 120 °C for 72 h to generate DDM as a bright yellow crystalline solid. The obtained crystalline solids were completely washed with water and MeOH and dried in air (201.6 mg, Yield: 85%). Anal. calcd for $[C_{66}H_{69}Br_3N_6]_n$: C,66.84; H, 5.86; N, 7.09. Found: C, 66.72; H, 5.97; N, 7.21. FT-IR (KBr, cm^{-1}): 3018, 2918, 2850, 1587, 1506, 1437, 1374, 1344, 1243, 1168, 1113, 1006, 806, 687.

1.5. Catalytic activity test

The cycloaddition of CO_2 with epoxides was performed in a 15 mL three-necked schlenk flask. In a typical run, the catalyst and epoxides were added into the reactor. The reactor was subsequently purged three times with CO_2 and then allowed to react for 5 hours at 90 °C under a pressure of 1 bar of CO_2. After the completion of the reaction, the liquid product was analyzed on a GC (Agilent GC-7890A, Agilent 19091J-413 capillary column, and FID detector). As PO is highly volatile, quantitative analysis of the product by the internal standard method is inaccurate. Hence, the GC quantitative analysis of the product is performed by the external standard method.

1.6. Recycle text

Recycle experiment was carried out under the optimal reaction conditions (reaction temperature 90 °C, 0.1 MPa CO_2 initial pressure, catalyst amount 2.5 mol%, reaction time 5 h). The $[Bn_2DMPz]Br$ was separated by column chromatography (eluent: petroleum ether/ethyl acetate, V/V = 1:1) from the reaction mixture. The product was flushed from the chromatographic column by the eluent while the $[Bn_2DMPz]Br$ was remained in the chromatographic column. $[Bn_2DMPz]Br$ in the chromatographic

column was dissolved with methanol. Then the mixture was filtered with a sand core funnel. Finally, the catalyst was collected after concentrating the filtrate.

The heterogeneous catalyst DDM was easily separated by centrifugation. After centrifugation, the solid catalysts were washed with water and acetonitrile and the combined organic solution was concentrated under reduced pressure followed by flash chromatography to give the desired product. The recovered catalyst was then washed with water and EtOH and dried at 80 °C under vacuum for 6 h before using for the next catalytic cycle.

1.7. Computational details

The structures of the reactants, intermediates, and transition states are optimized by the B3PW91[1,2] method and 6-31G(d,p) basis set[3]. The energies are refined at four functionals (M06, B3PW91, MN15, and B3LYP-D3) with the larger 6-311+G(2d,2p) basis set on optimized geometries at the level of B3PW91/6-31G(d,p). The solvent effect is taken into account by the polarized continuum model (PCM)[4,5] and the substrate epichlorohydrin is selected as solvent [Eps = 22.6 and EpsInf = 2.062]. Based on the calculated relative free energies (Table S1), it shows that the dispersion corrected density functional B3LYP-D3 is more reliable due to the resonable activation energies and reaction energy (−2.3). In contrast, the reaction free energy of the whole coupling of CO_2 with epoxide to form cyclic carbonate at the M06 and B3PW91 levels is predicted to be endergic by 2.4 and 8.0 kcal/mol, which shows that M06 and B3PW91 functionals are not unsuitable for this study. Above mentioned calculations were carried out by using the Gaussian 09 program package [M. J. Frisch, G W Trucks, H. B. Schlegel, et al. Gaussian 09, Revision E.01; Gaussian, Inc., Wallingford, CT, 2013.].

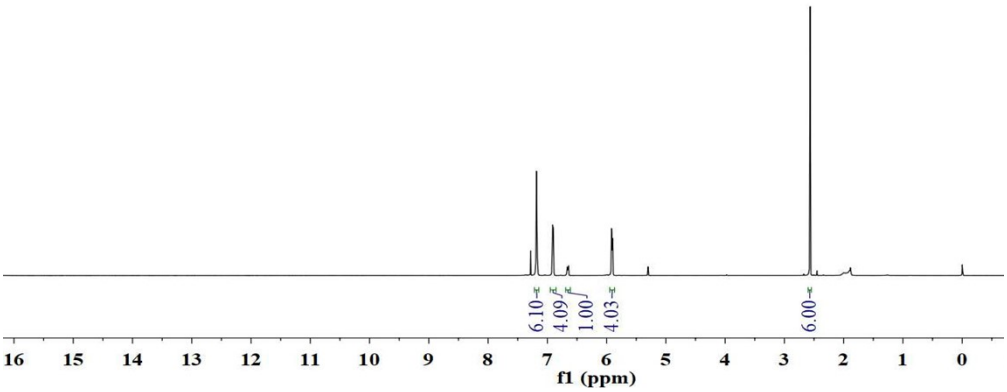

Fig. S1. ^{1}H NMR for **8** ($CDCl_3$, 600 MHz).

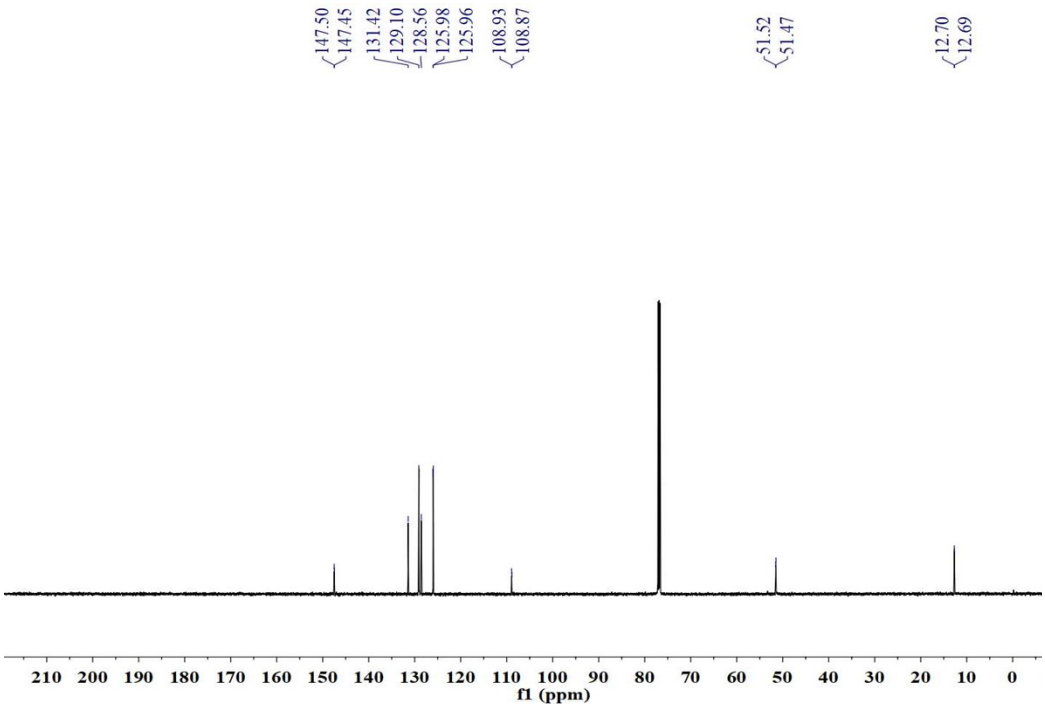

Fig. S2. ^{13}C NMR for **8** ($CDCl_3$, 151 MHz).

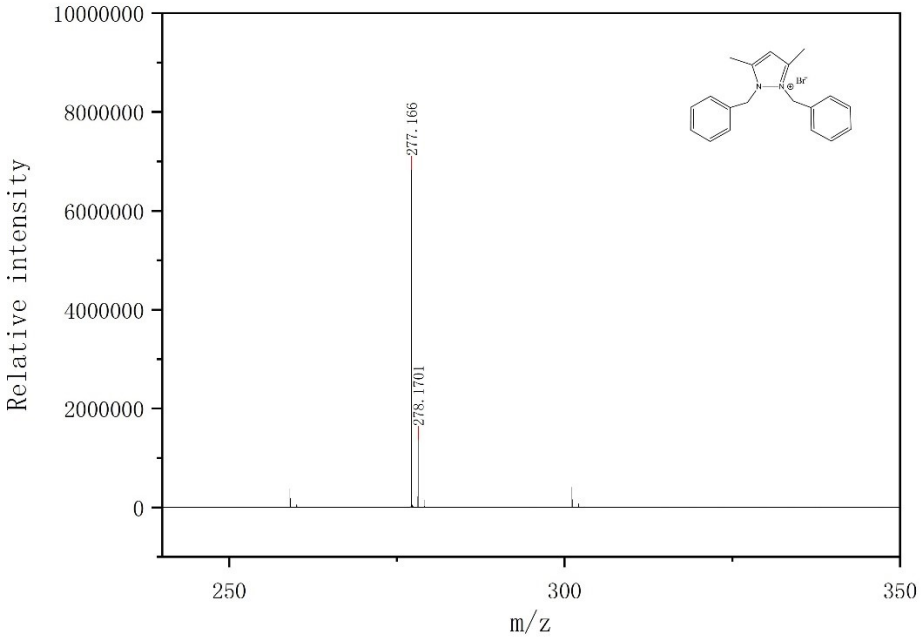

Fig. S3. HR-MS (QTOF) for **8**.

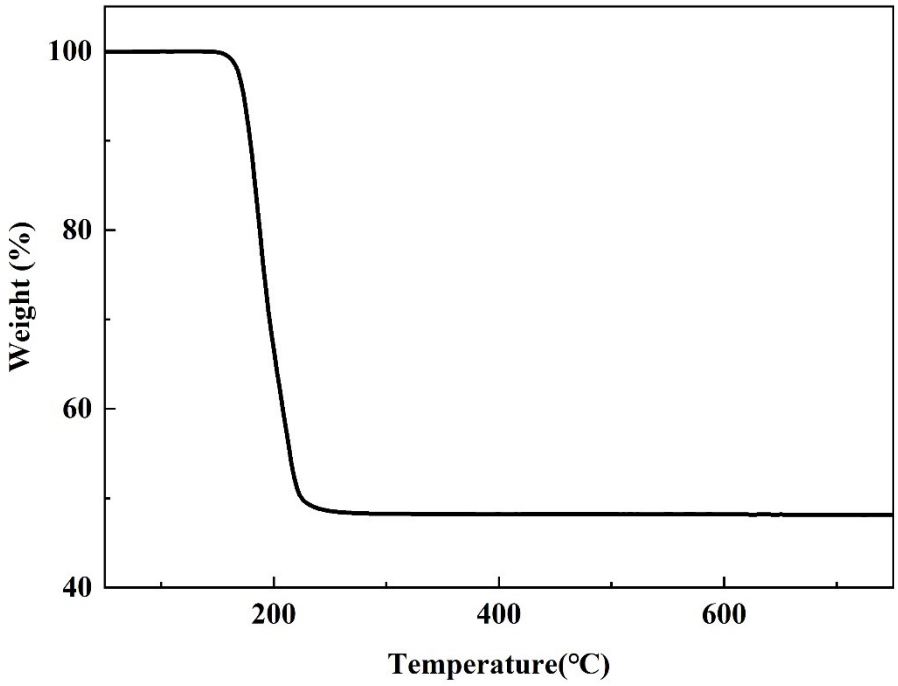

Fig. S4. TGA curve of **8**. The compound starts to decompose at 167 °C.

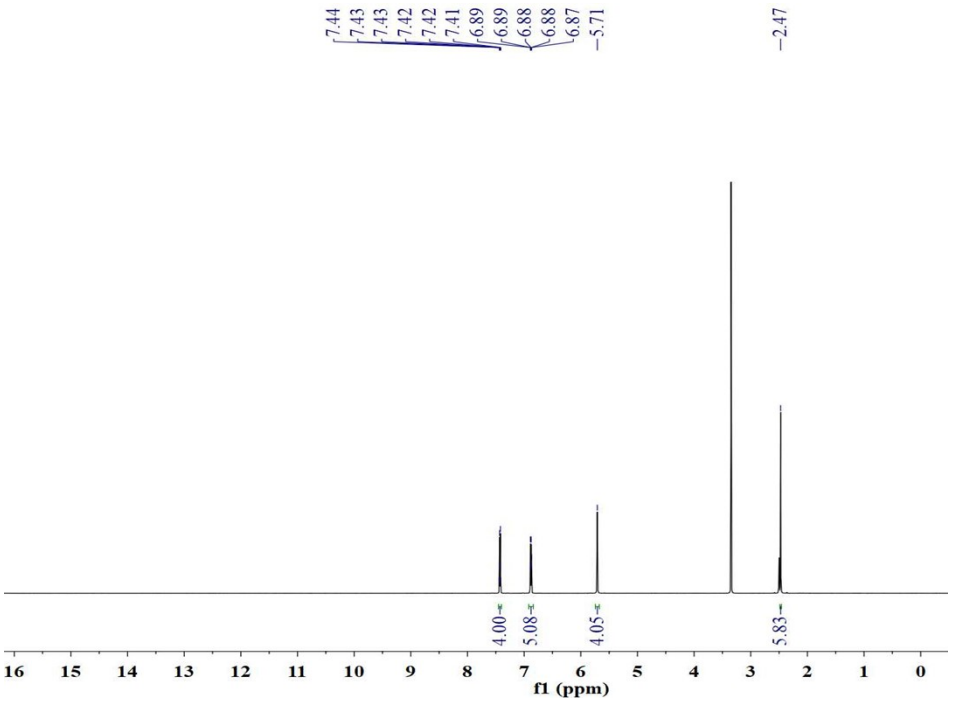

Fig. S5. ^{1}H NMR for **9** (DMSO, 600 MHz).

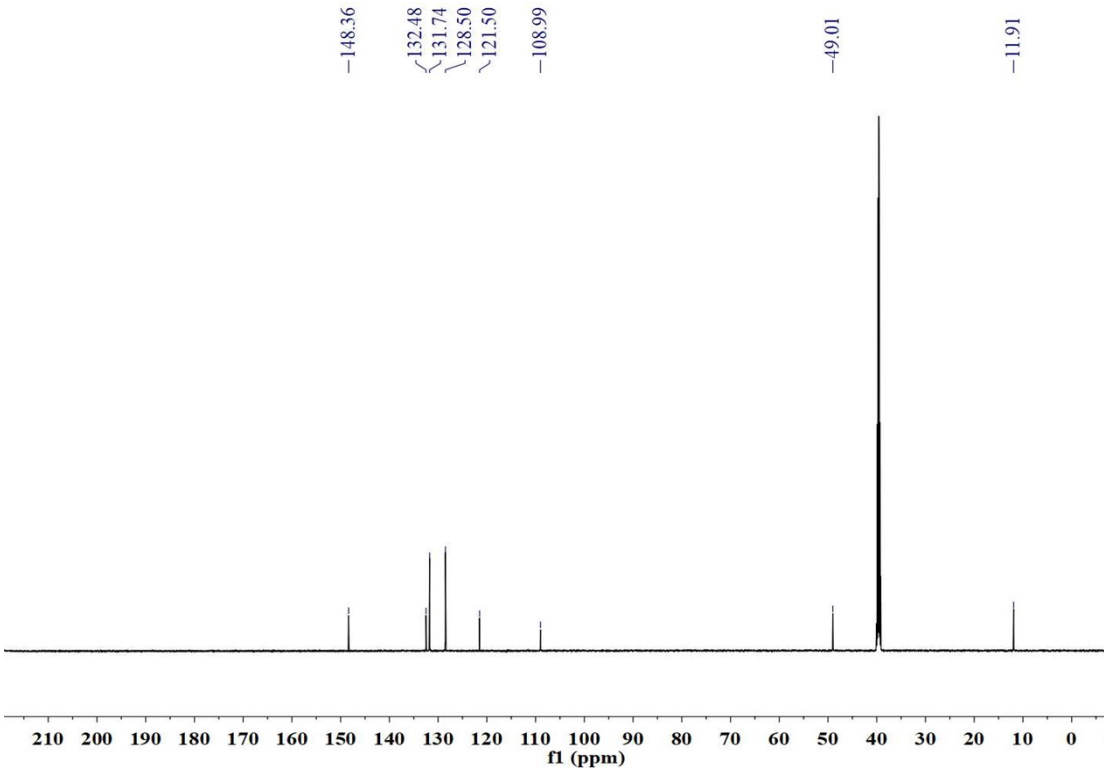

Fig. S6. ^{13}C NMR for **9** (DMSO, 151 MHz).

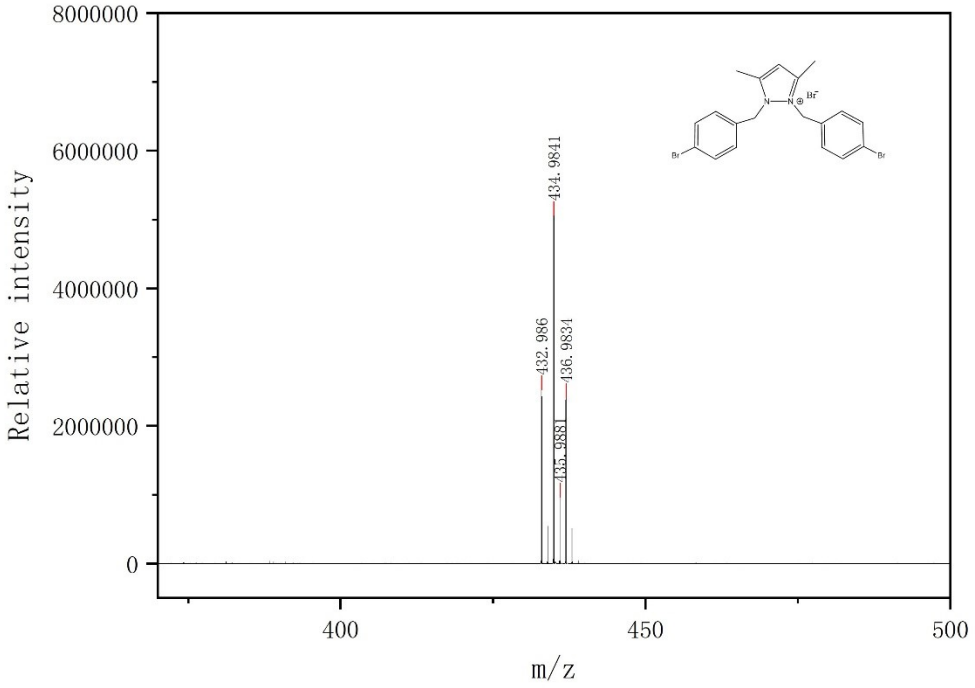

Fig. S7. HR-MS (QTOF) for **9**.

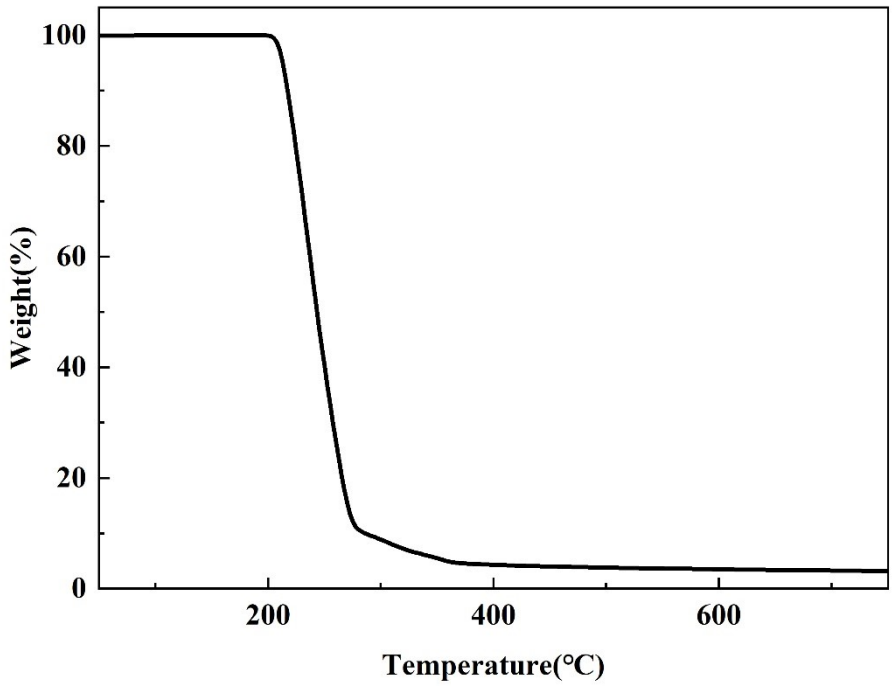

Fig. S8. TGA curve of **9**. The compound starts to decompose at 203 °C.

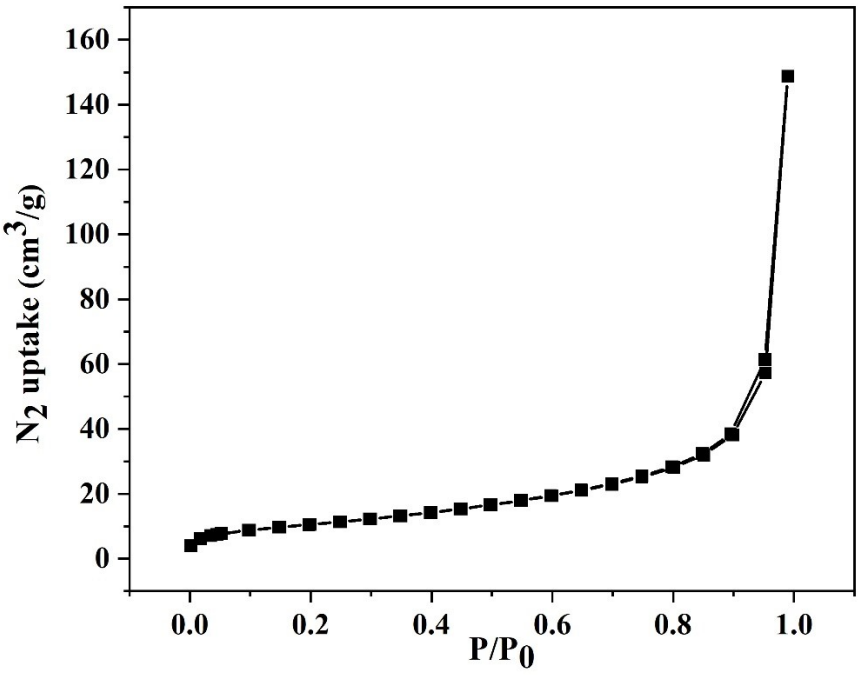

Fig. S9. N_2 adsorption (filled) and desorption (open) isotherm profiles of DDP.

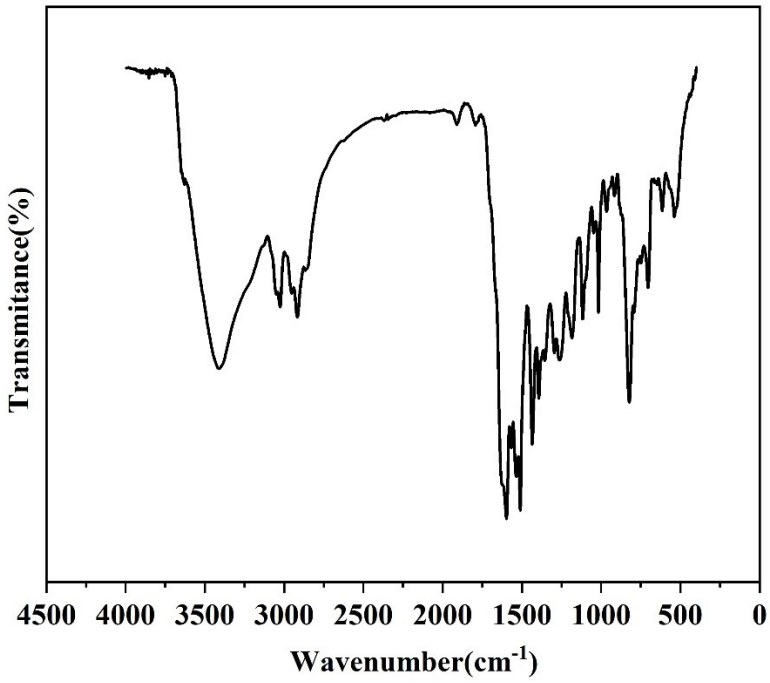

Fig. S10. FT-IR spectra of DDP.

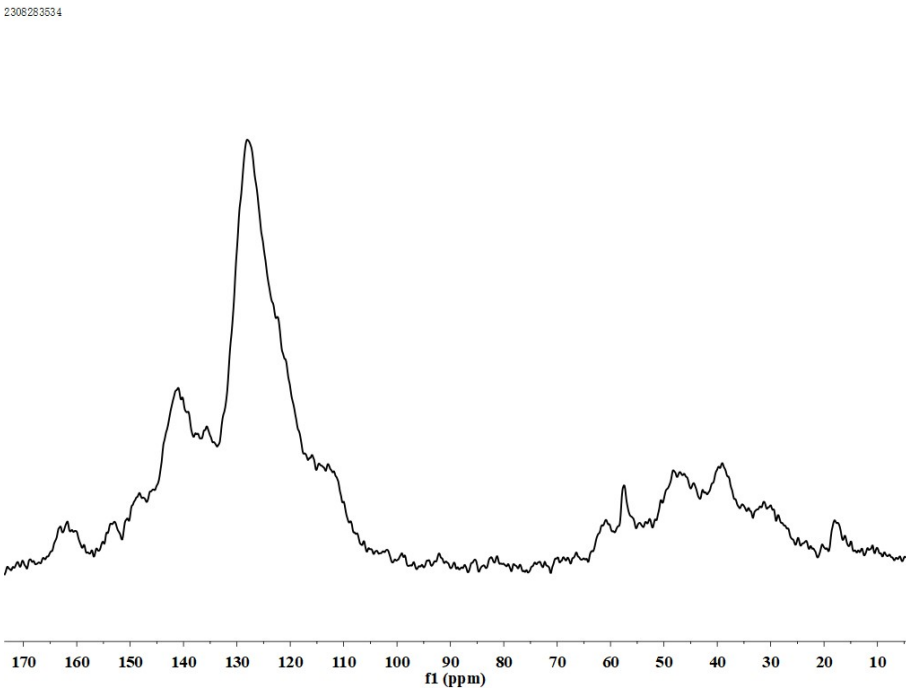

Fig. S11. Solid state ^{13}C CP/MAS NMR spectroscopy of DDP.

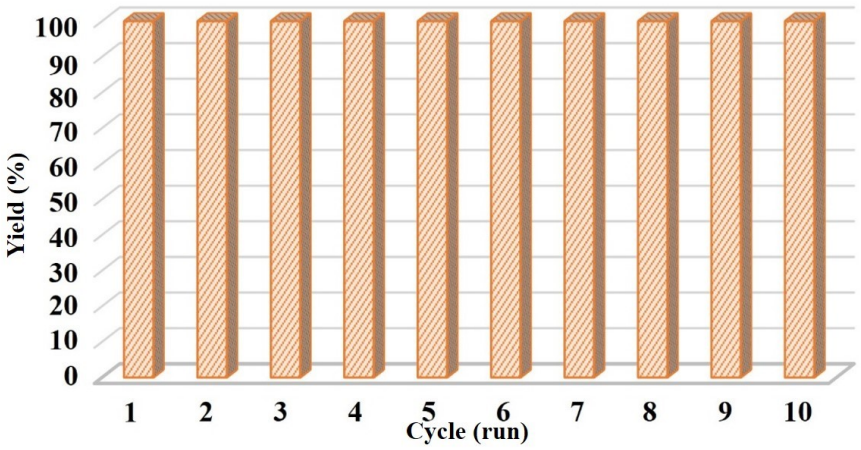

Fig. S12. Catalytic recycling test of DDP with epichlorohydrin and CO_2 ((Reaction conditions: PO 40 mmol, catalyst amount 0.6 mol%, reaction time 7.0 h, temperature 120 °C, DMF (1.0 mL) as solvent.).

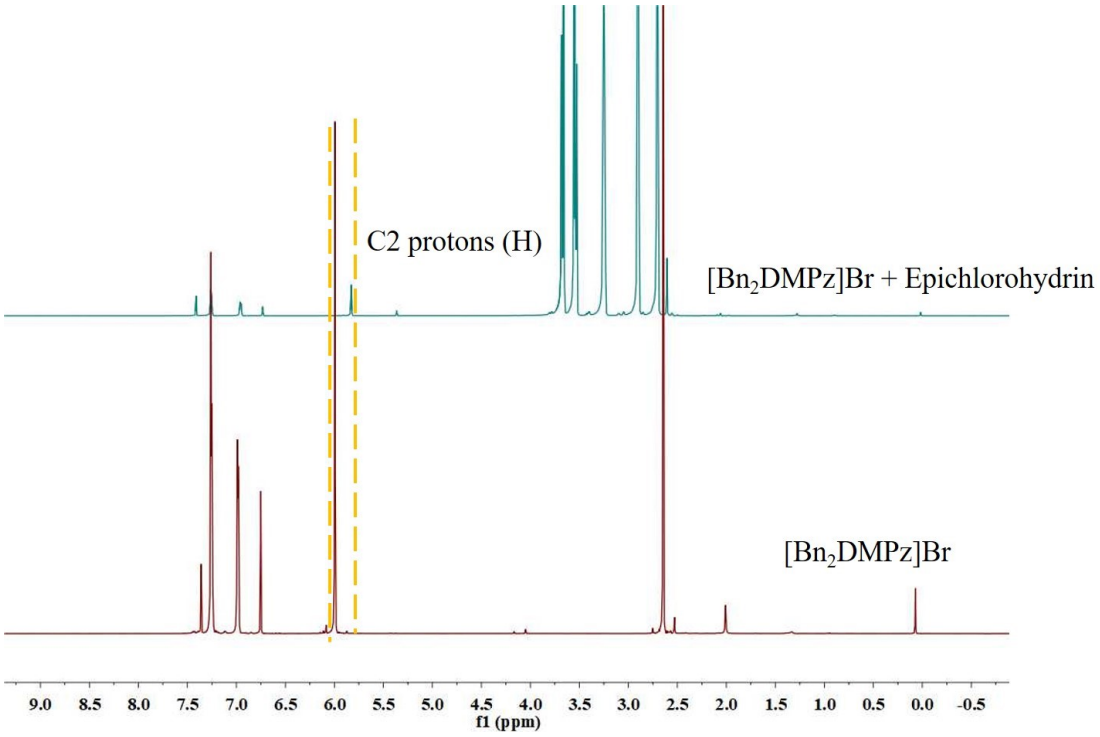

Fig. S13. The comparison of the 1H NMR spectrum of [Bn_2DMPz]Br and the mixture of [Bn_2DMPz]Br and epichlorohydrin.

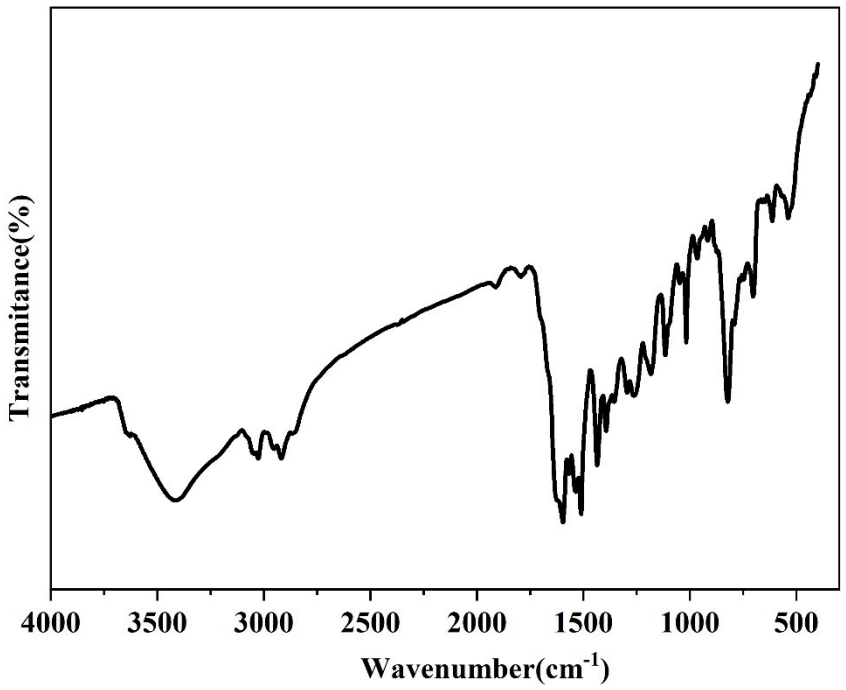

Fig. S14. FT-IR spectra of 10rd DDP.

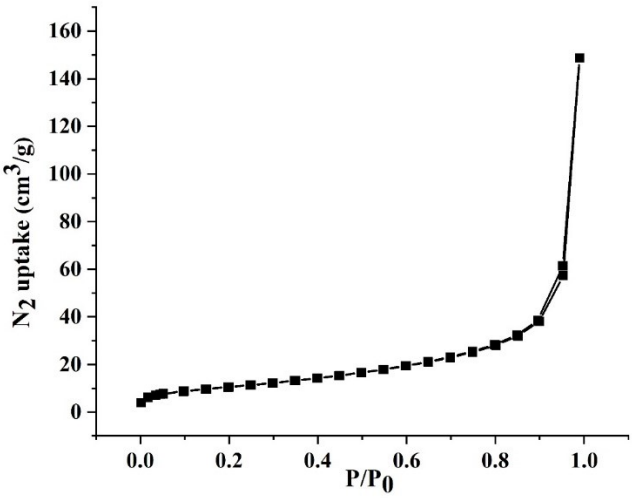

Fig. S15. N_2 adsorption (filled) and desorption (open) isotherm profiles of 10rd DDP.

Table S1. The relative Gibbs free energies (kcal/mol) of crucial stationary points involved in "Single-IL" mechanism calculated by different functionals.

	M06	B3LYP-D3	MN15	B3PW91
TS1	**32.0**	27.1	33.3	37.8
1a	**23.5**	18.1	30.2	28.0
2a	**16.2**	13.7	16.1	6.9
TS2	**31.2**	24.6	27.0	19.2
PC	**4.5**	−0.8	−1.9	−8.9

Table S2. The relative Gibbs free energies (kcal/mol) of crucial stationary points involved in "Double-IL" mechanism calculated by different functionals.

	M06	B3LYP-D3	MN15	B3PW91
TS1	**30.0**	26.1	31.3	31.6
1a	**22.9**	22.8	27.9	29.5
2a	**18.5**	17.2	15.8	25.5
TS2	**32.0**	26.3	26.1	34.2
PC	**2.0**	−2.3	−6.2	8.4

GC spectra

A：[Bn_2DMPz]Br as a homogeneous catalyst

reactant

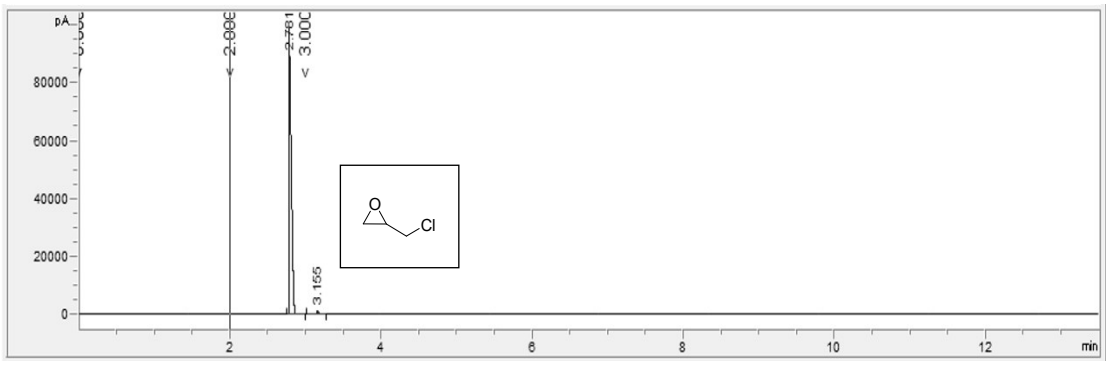

product

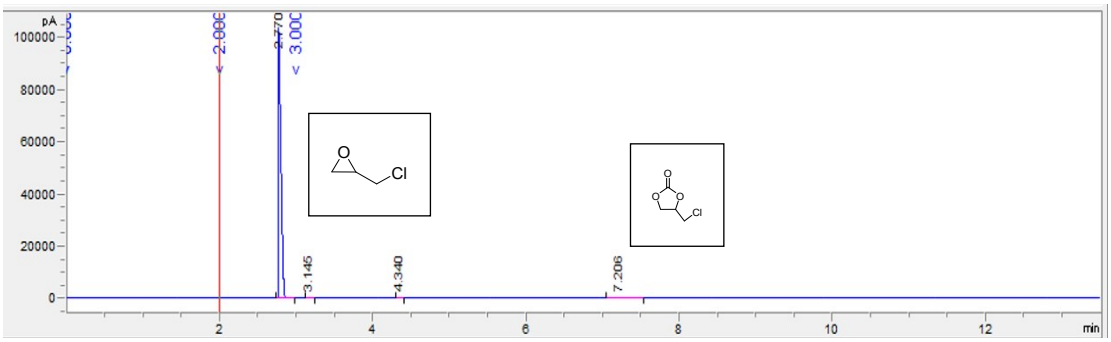

reactant

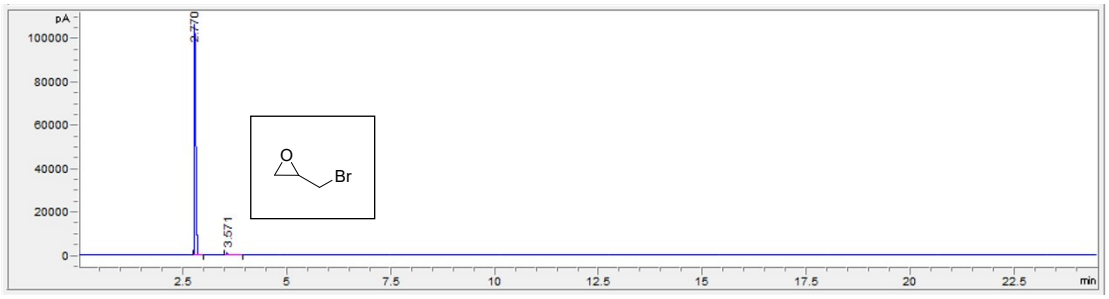

product

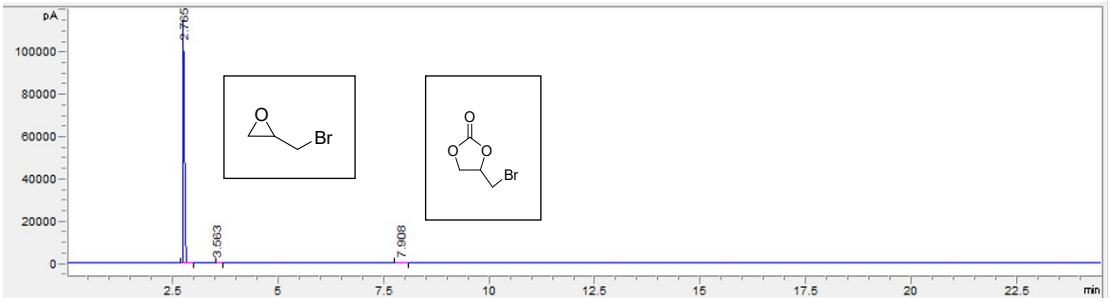

reactant

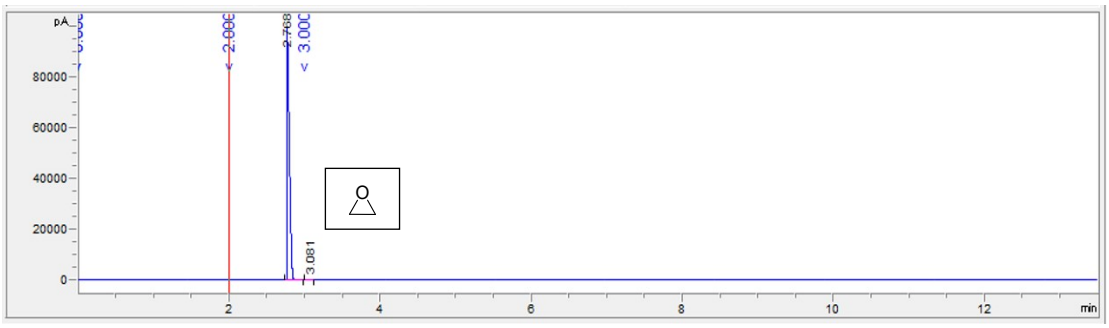

product

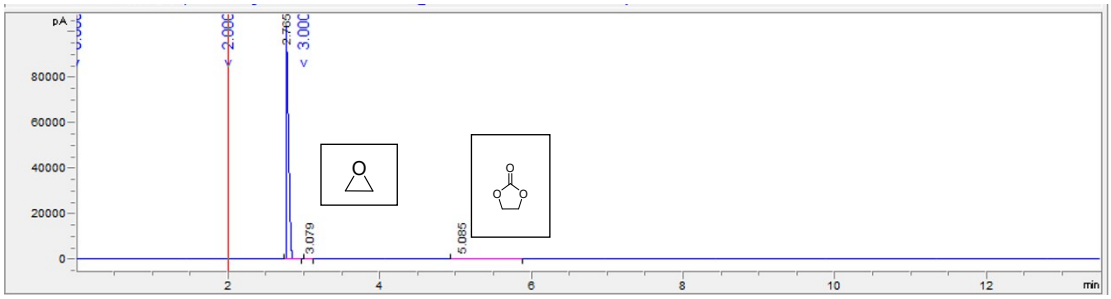

reactant

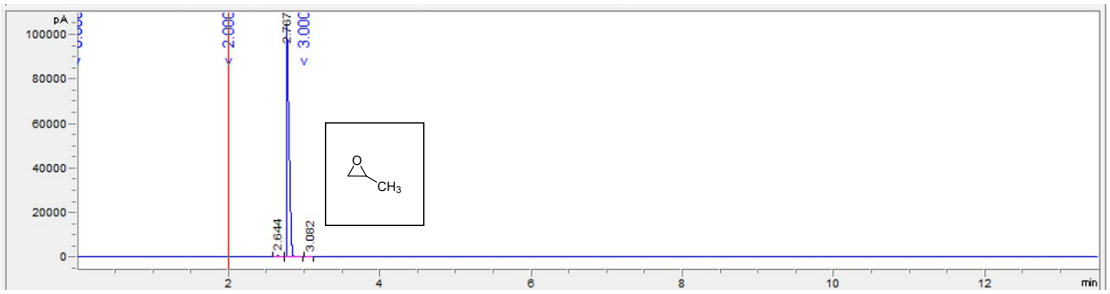

product

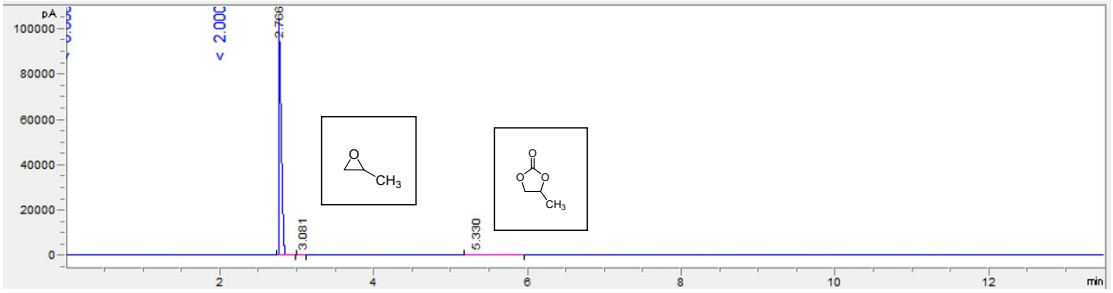

reactant

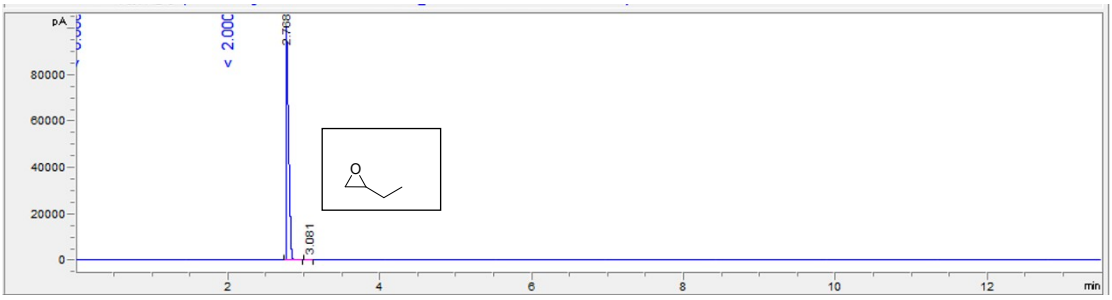

product

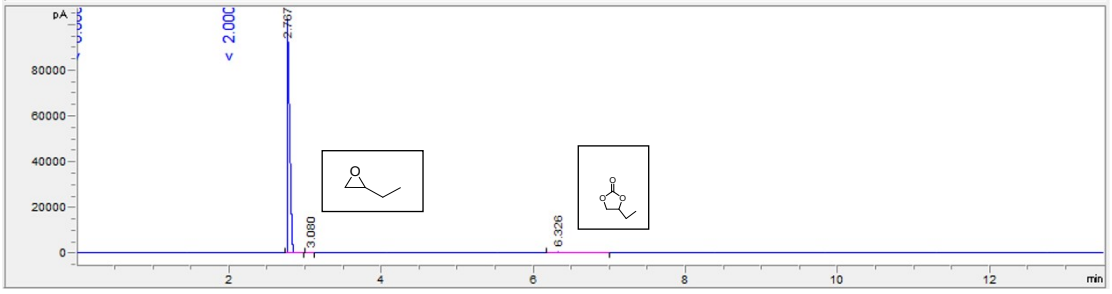

reactant

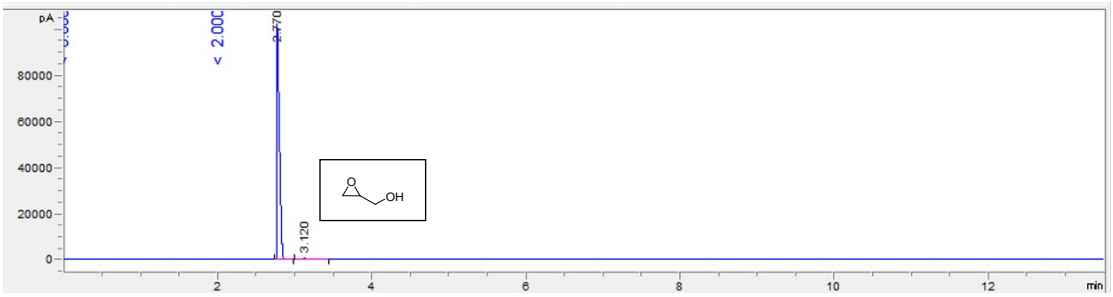

product

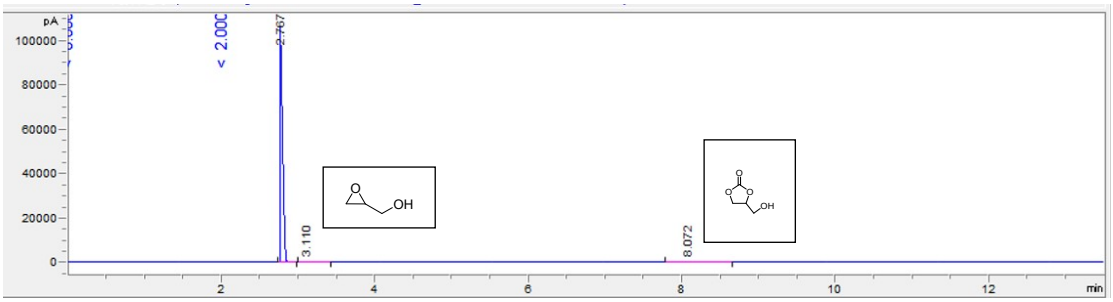

reactant

product

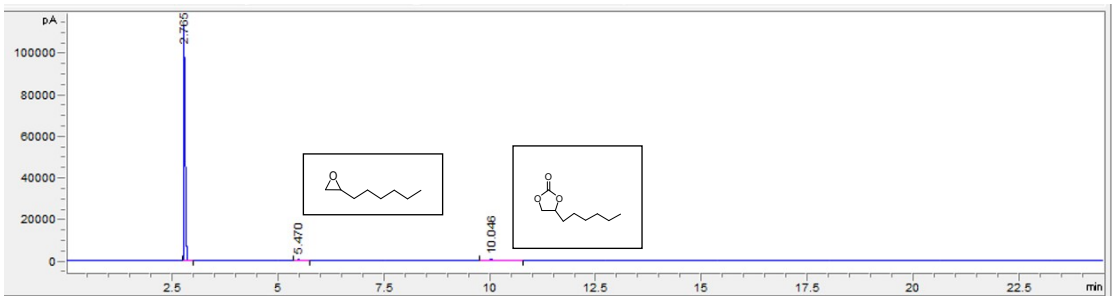

reactant

product

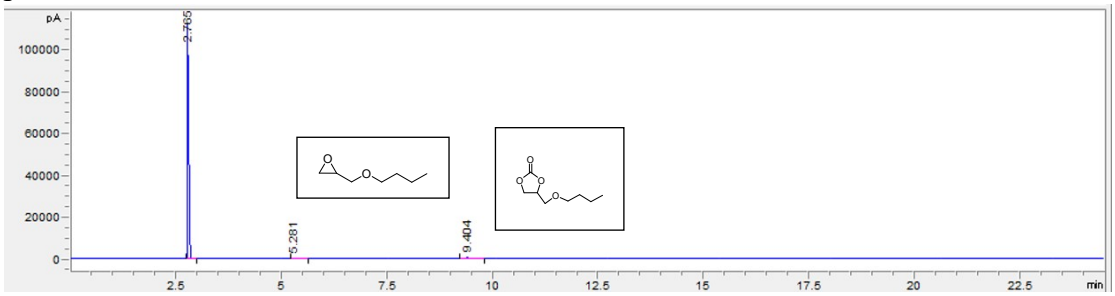

reactant

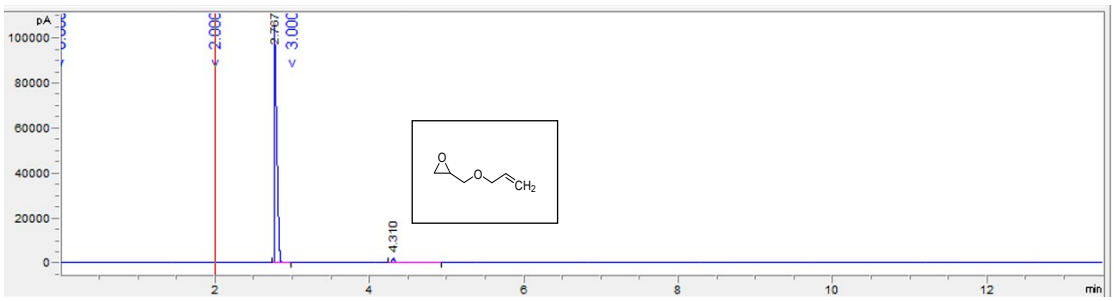

product

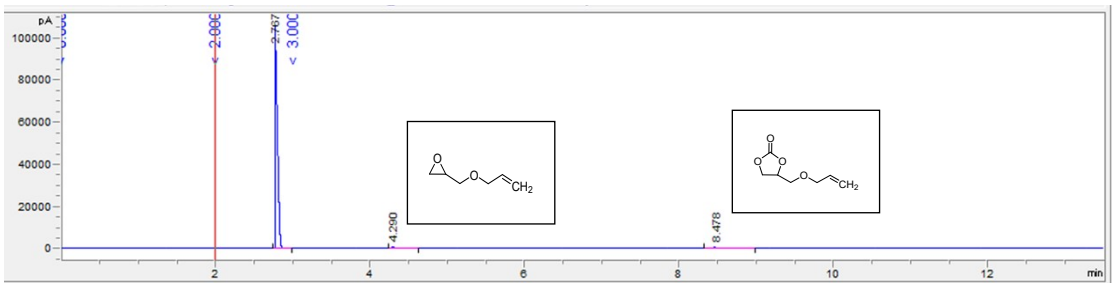

reactant

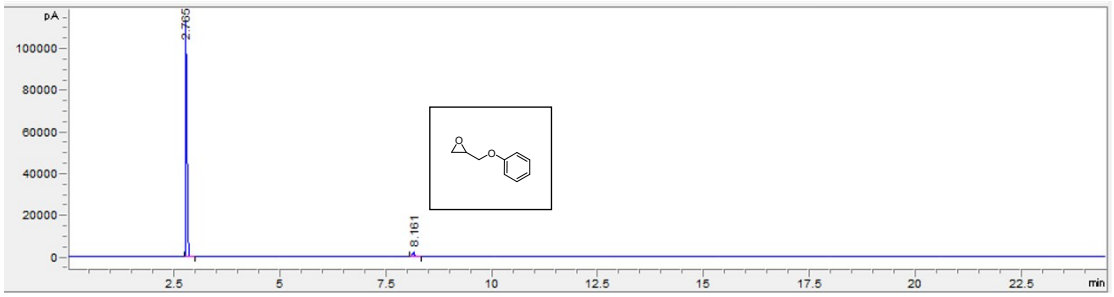

product

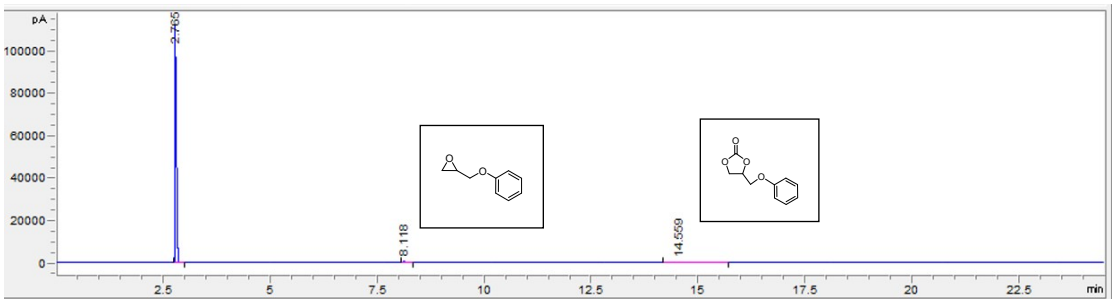

reactant

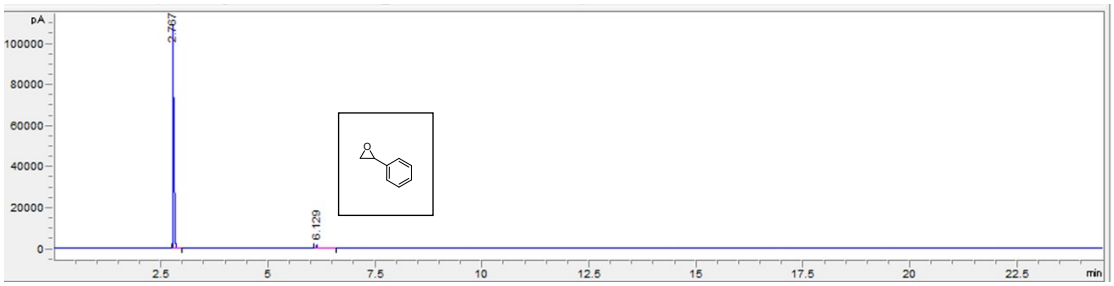

product

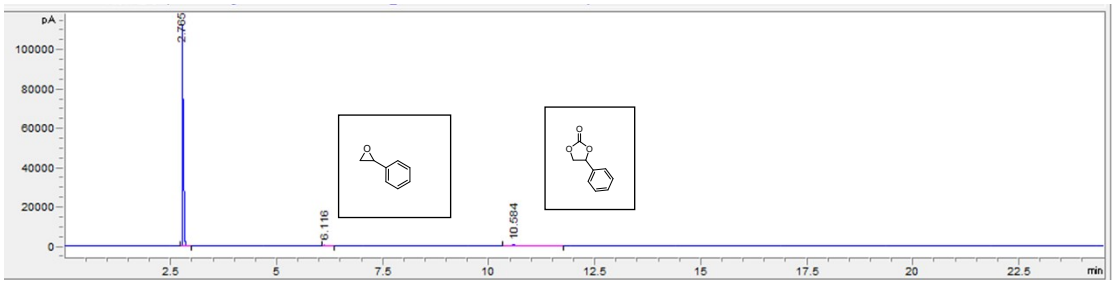

reactant

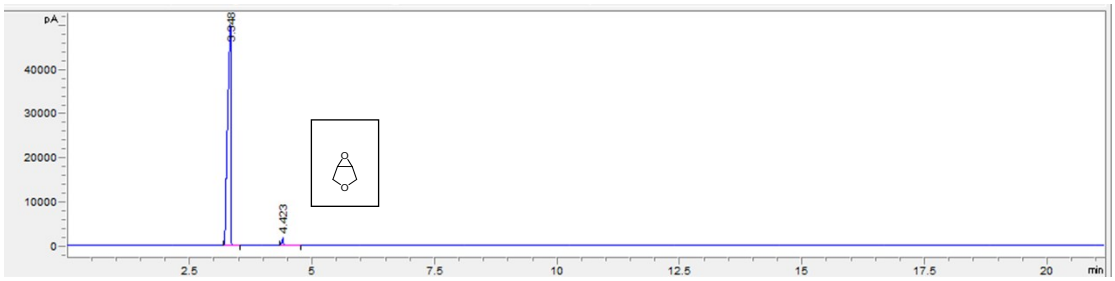

product

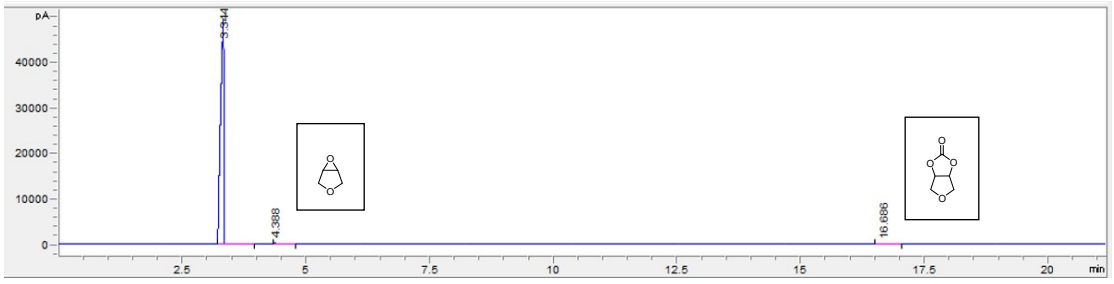

B：DDP as a heterogeneous catalyst

reactant

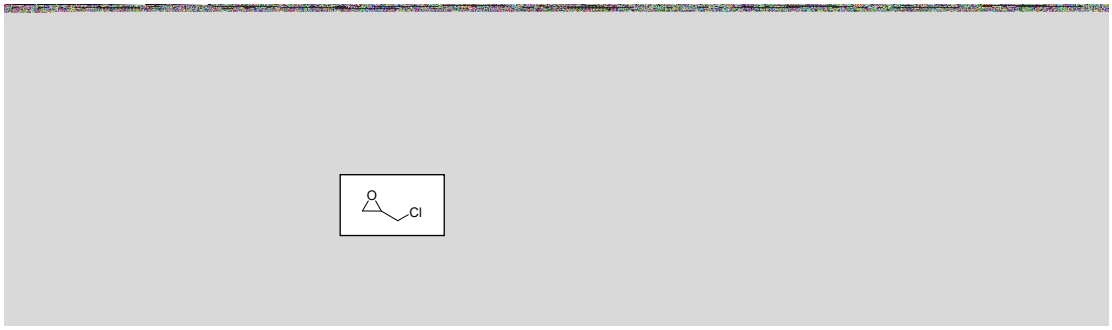

product

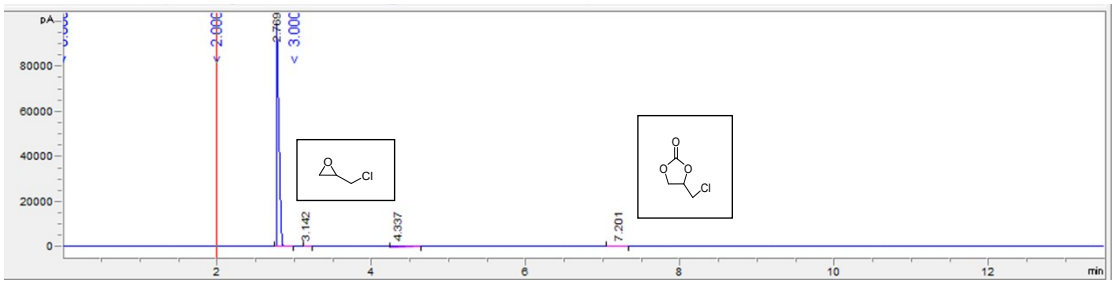

reactant

product

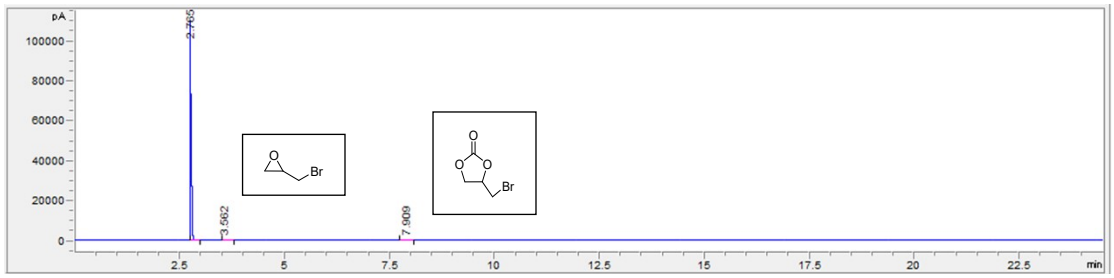

reactant

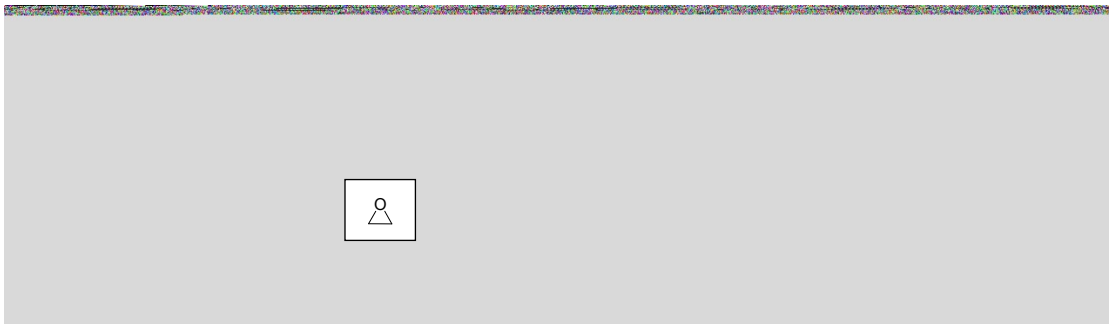

product

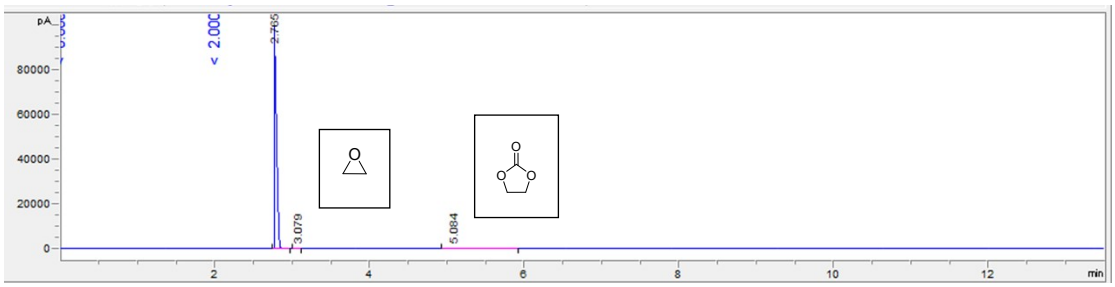

reactant

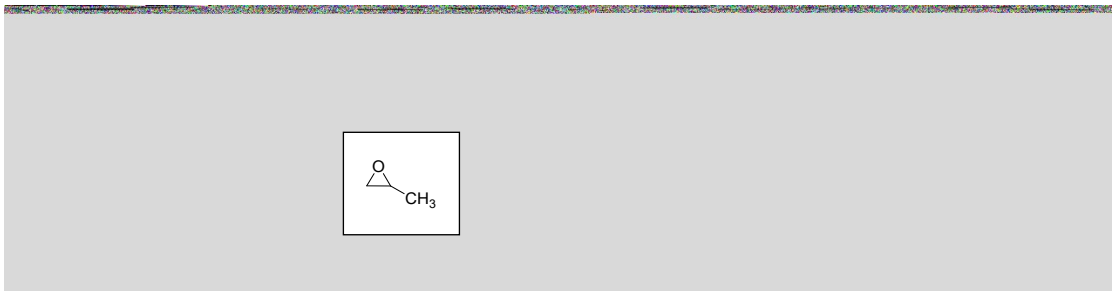

product

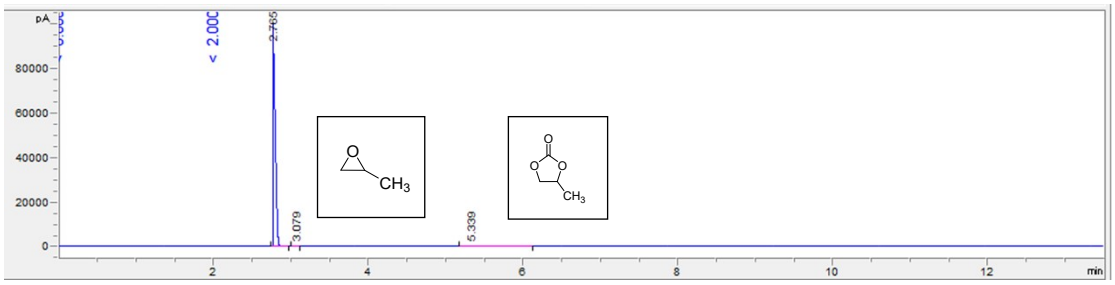

reactant

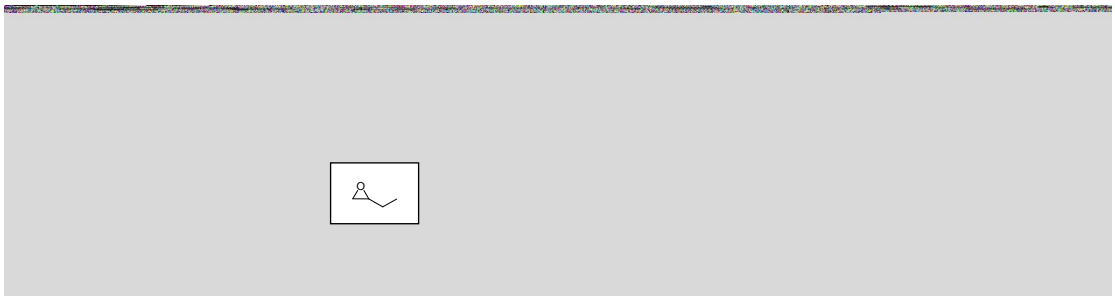

product

reactant

product

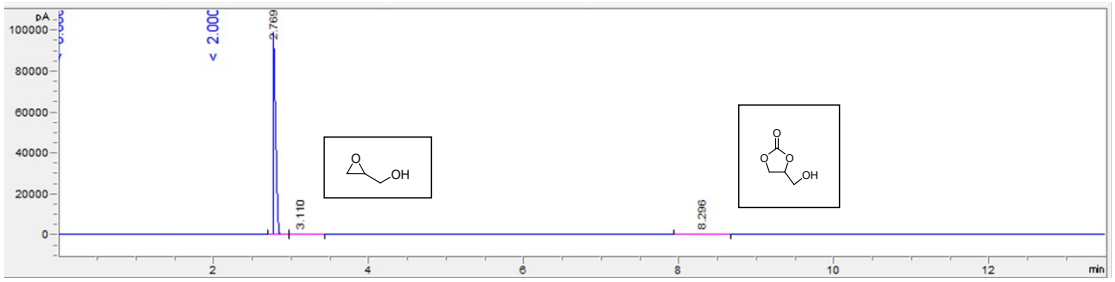

reactant

product

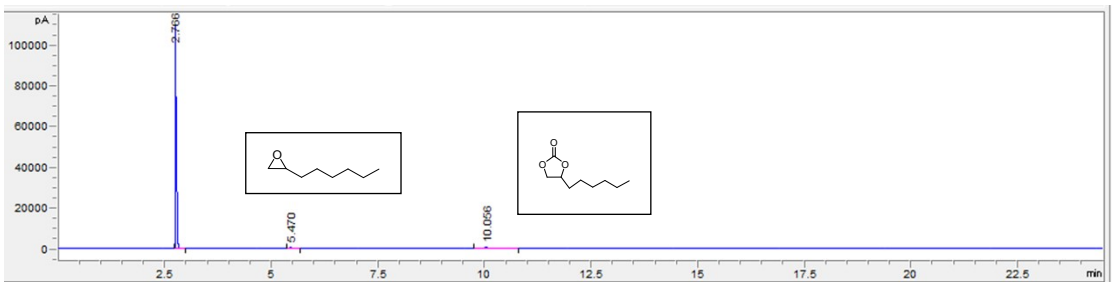

reactant

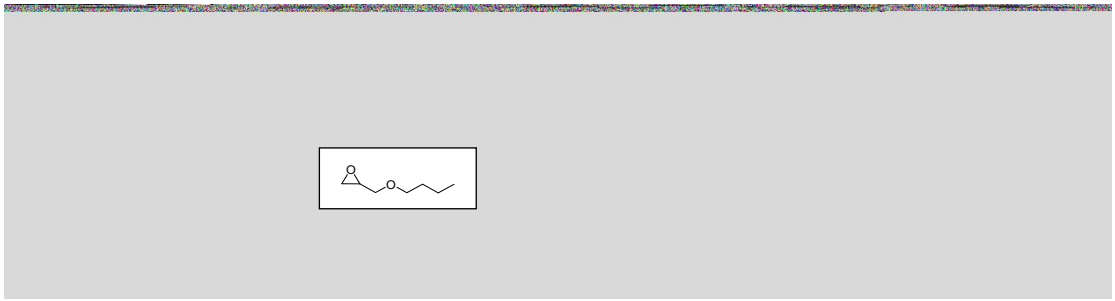

product

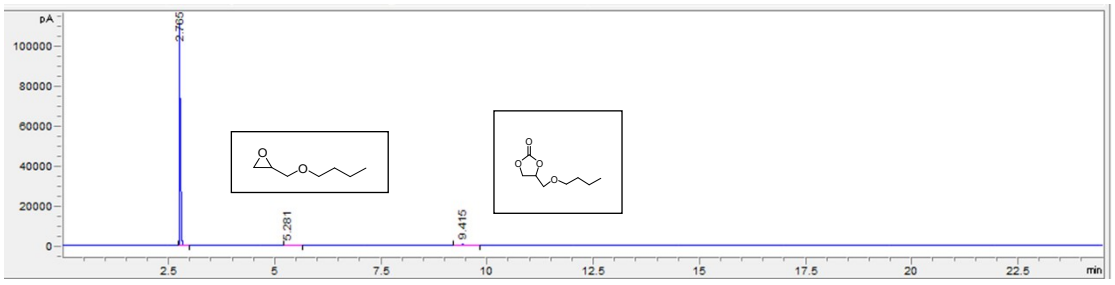

reactant

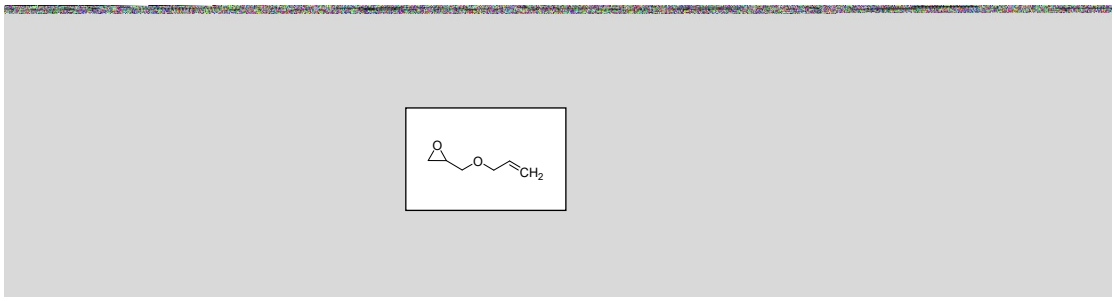

product

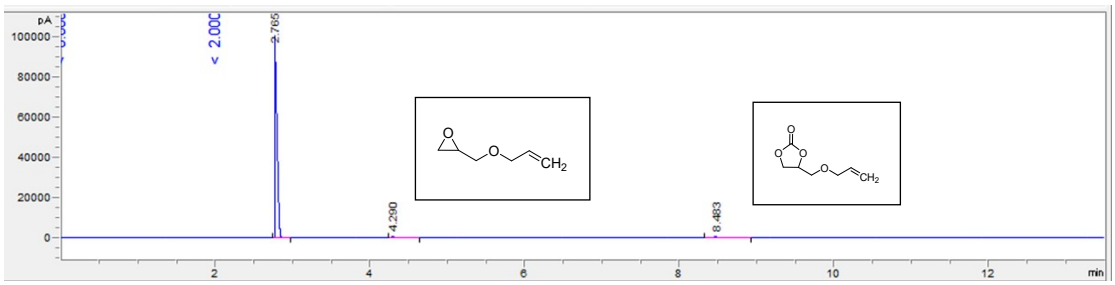

reactant

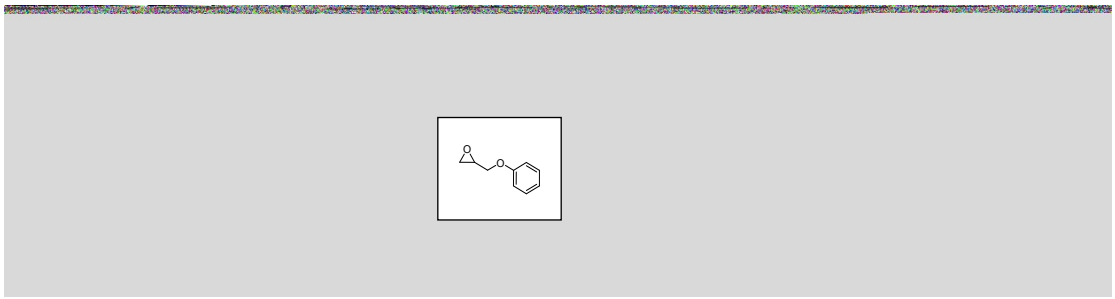

product

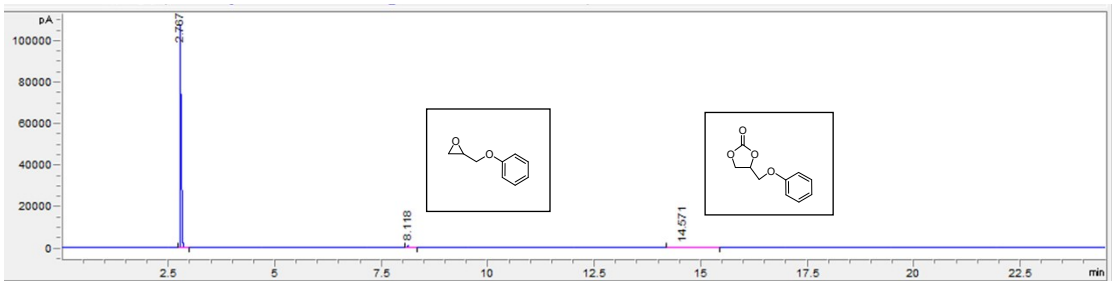

reactant

product

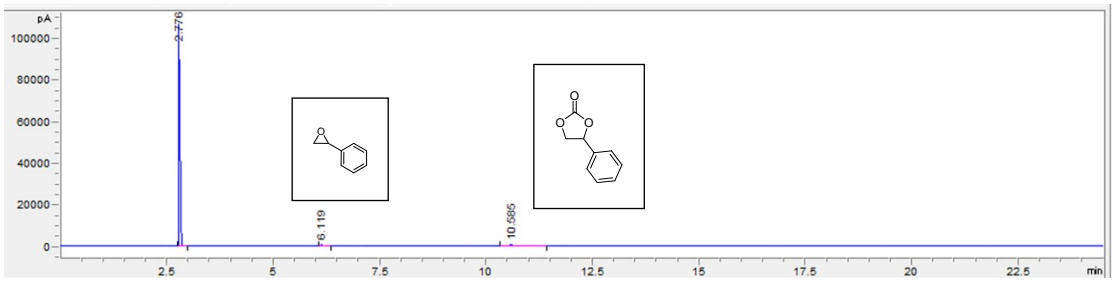

reactant

product

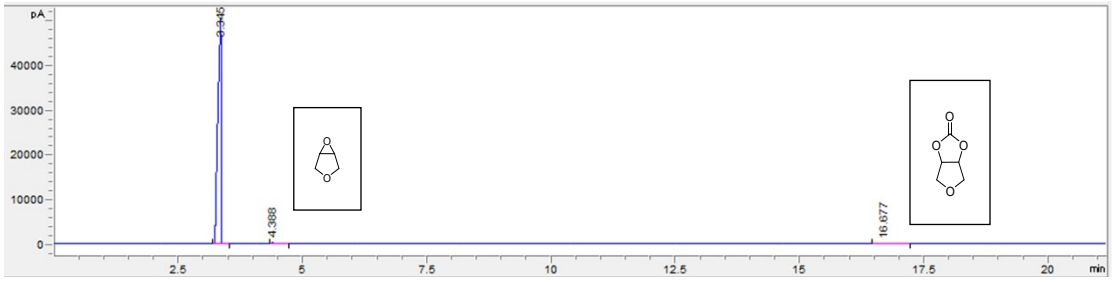

1a

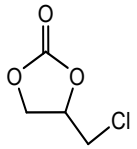
O
O
O
Cl

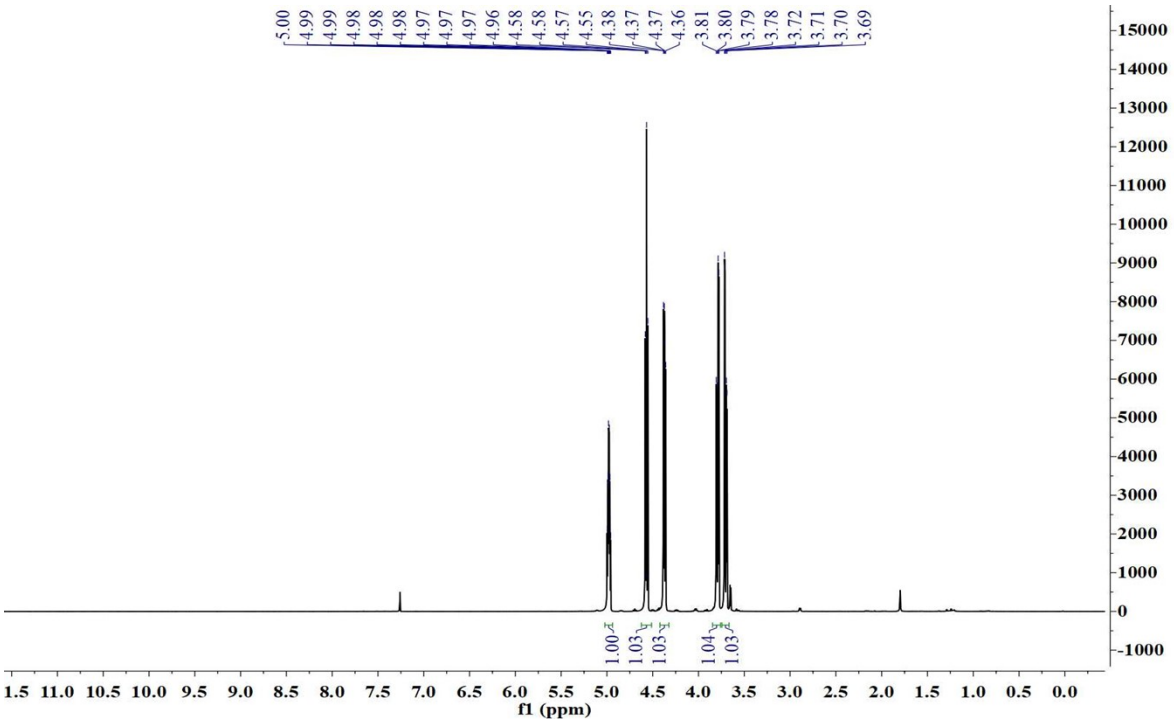
5.00
4.99
4.99
4.98
4.98
4.98
4.97
4.97
4.97
4.96
4.58
4.58
4.57
4.55
4.38
4.37
4.37
4.36
3.81
3.80
3.79
3.78
3.72
3.71
3.70
3.69
15000
14000
13000
12000
11000
10000
9000
8000
7000
6000
5000
4000
3000
2000
1000
0
-1000
1.00
1.03
1.03
1.04
1.03
1.5 11.0 10.5 10.0 9.5 9.0 8.5 8.0 7.5 7.0 6.5 6.0 5.5 5.0 4.5 4.0 3.5 3.0 2.5 2.0 1.5 1.0 0.5 0.0
f1 (ppm)

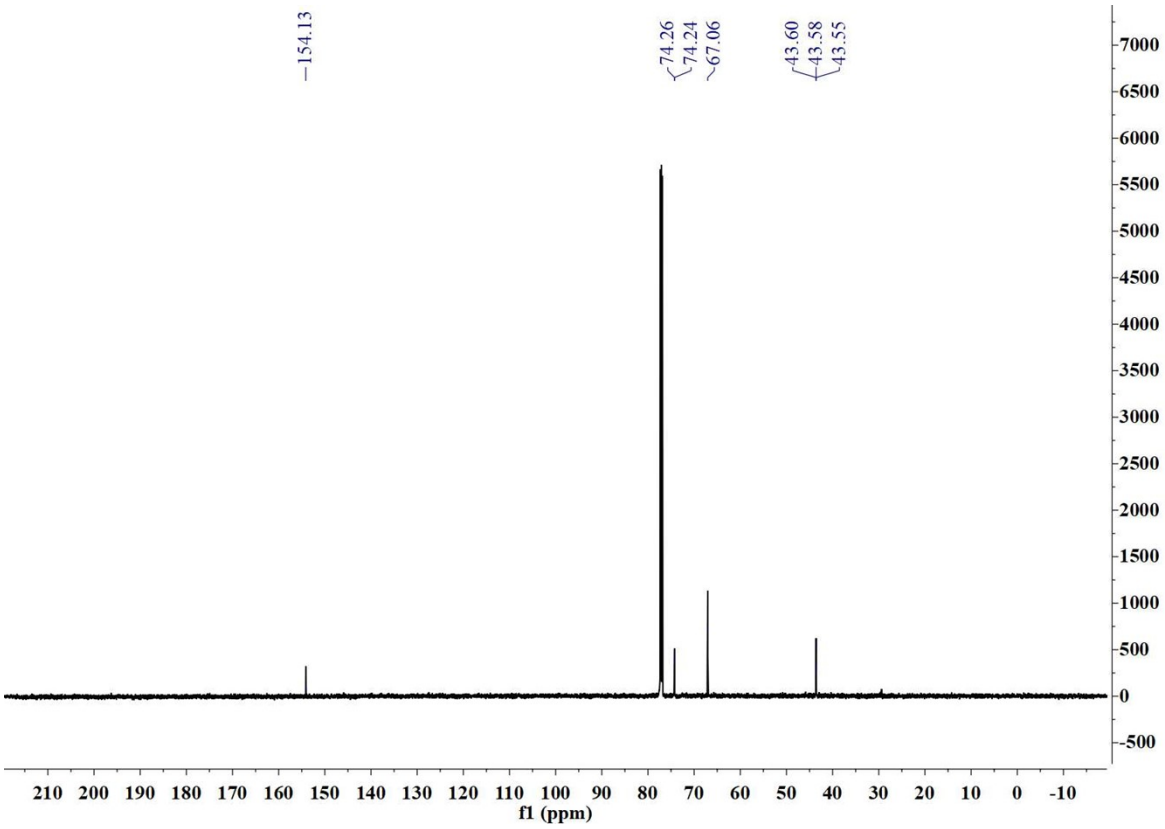
154.13
74.26
74.24
67.06
43.60
43.58
43.55
f1 (ppm)

1b

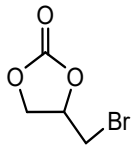
O
O
O
Br

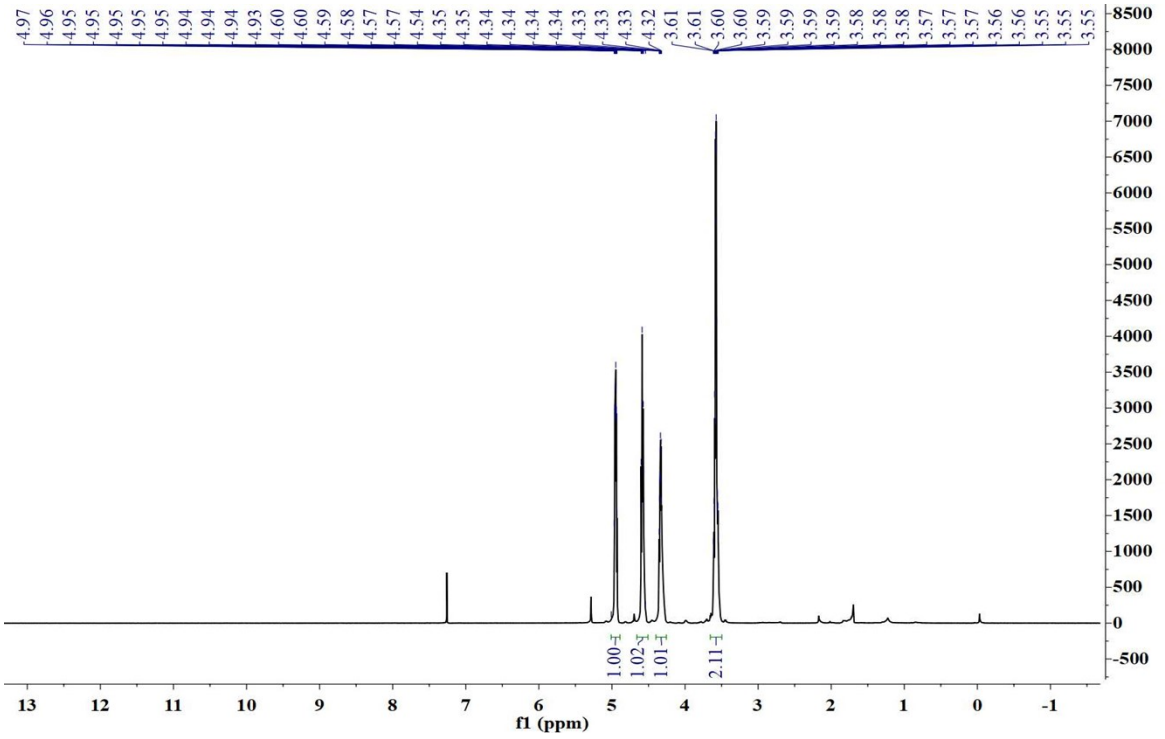
1.00
1.02
1.01
2.11
f1 (ppm)

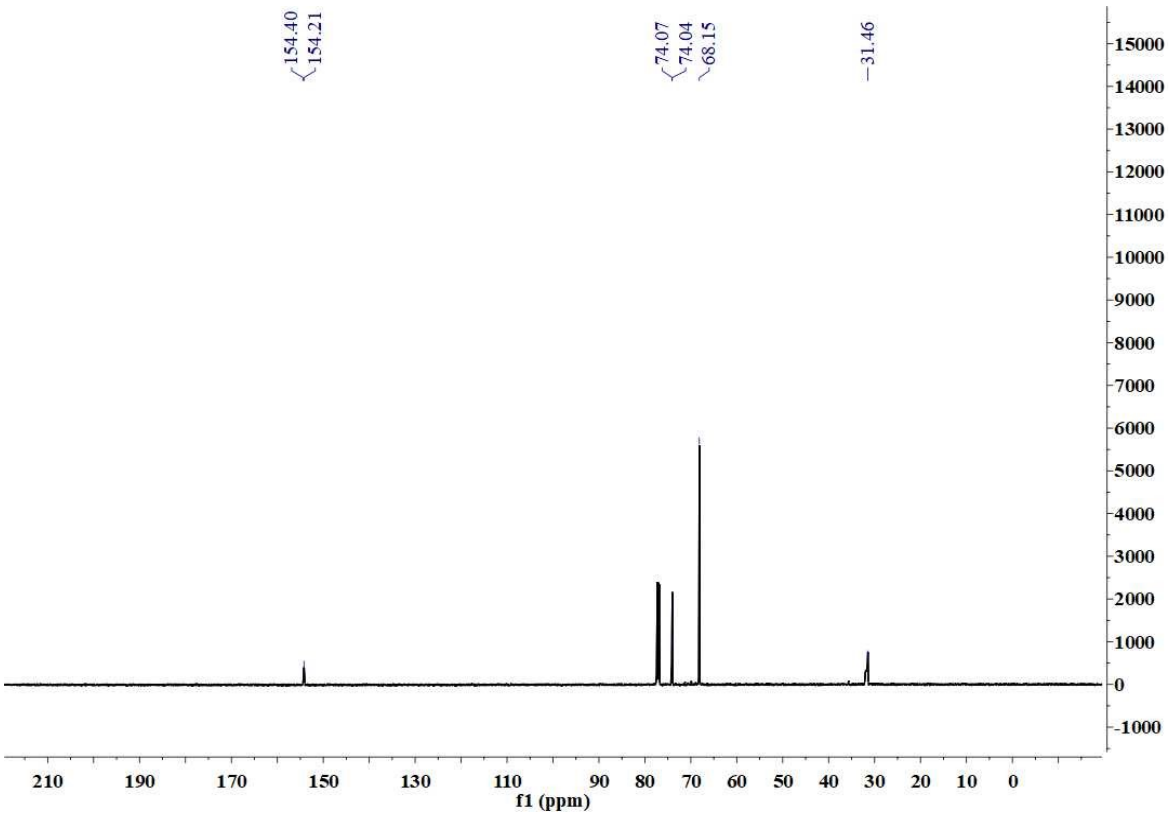
154.40
154.21
74.07
74.04
68.15
31.46
15000
14000
13000
12000
11000
10000
9000
8000
7000
6000
5000
4000
3000
2000
1000
0
-1000
210 190 170 150 130 110 90 80 70 60 50 40 30 20 10 0
f1 (ppm)

1c

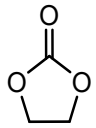

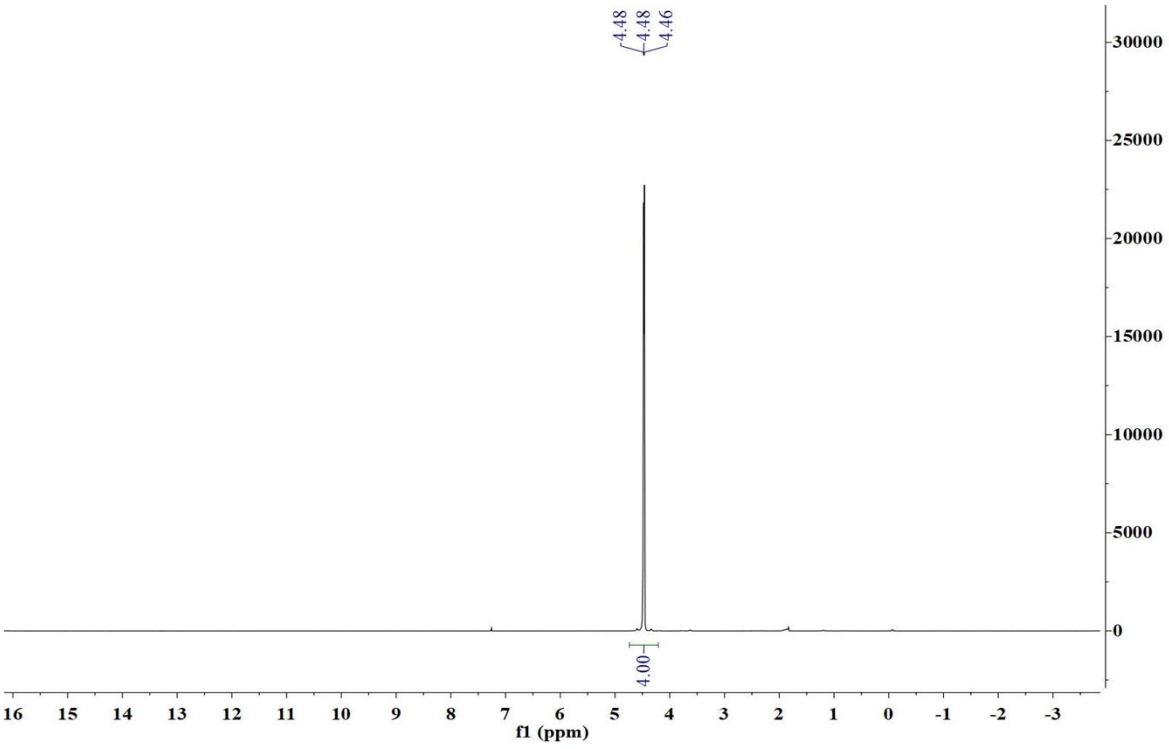
4.48
4.48
4.46
30000
25000
20000
15000
10000
5000
0
4.00
16 15 14 13 12 11 10 9 8 7 6 5 4 3 2 1 0 -1 -2 -3
f1 (ppm)

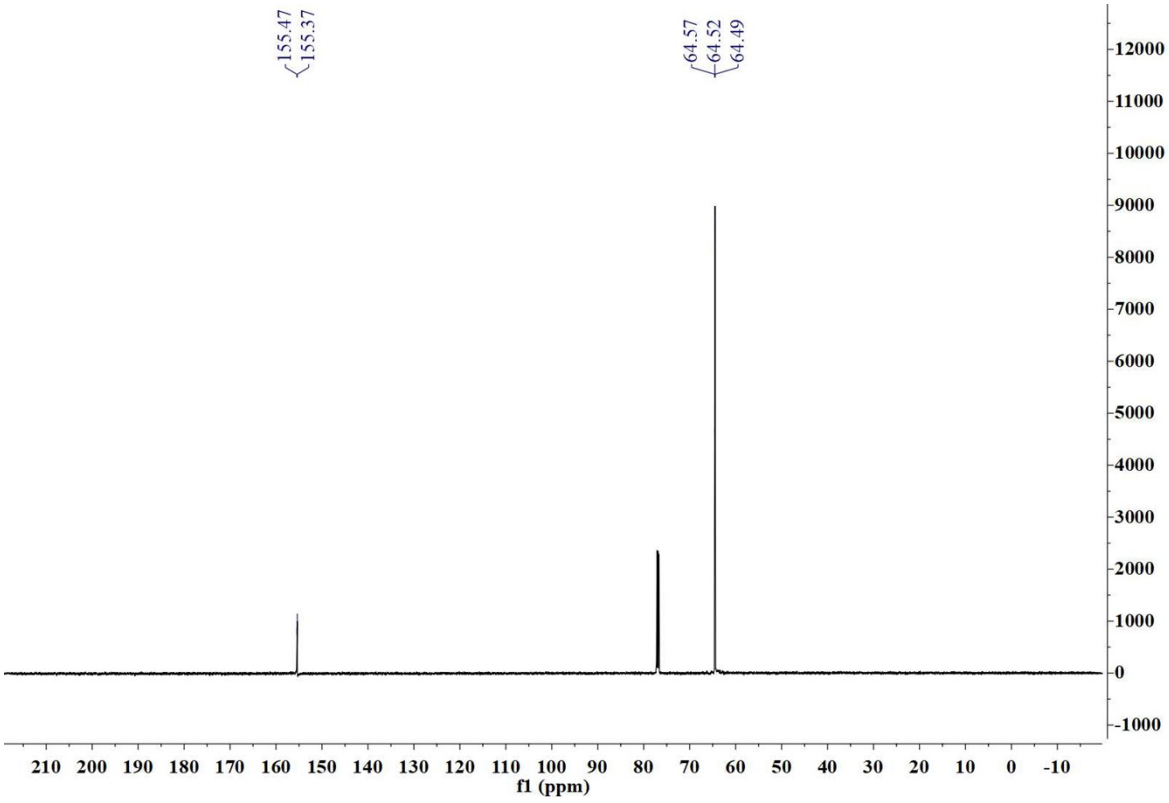
155.47
155.37
64.57
64.52
64.49
12000
11000
10000
9000
8000
7000
6000
5000
4000
3000
2000
1000
0
-1000
210 200 190 180 170 160 150 140 130 120 110 100 90 80 70 60 50 40 30 20 10 0 -10
f1 (ppm)

1d

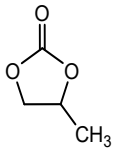
O
O
O
CH3

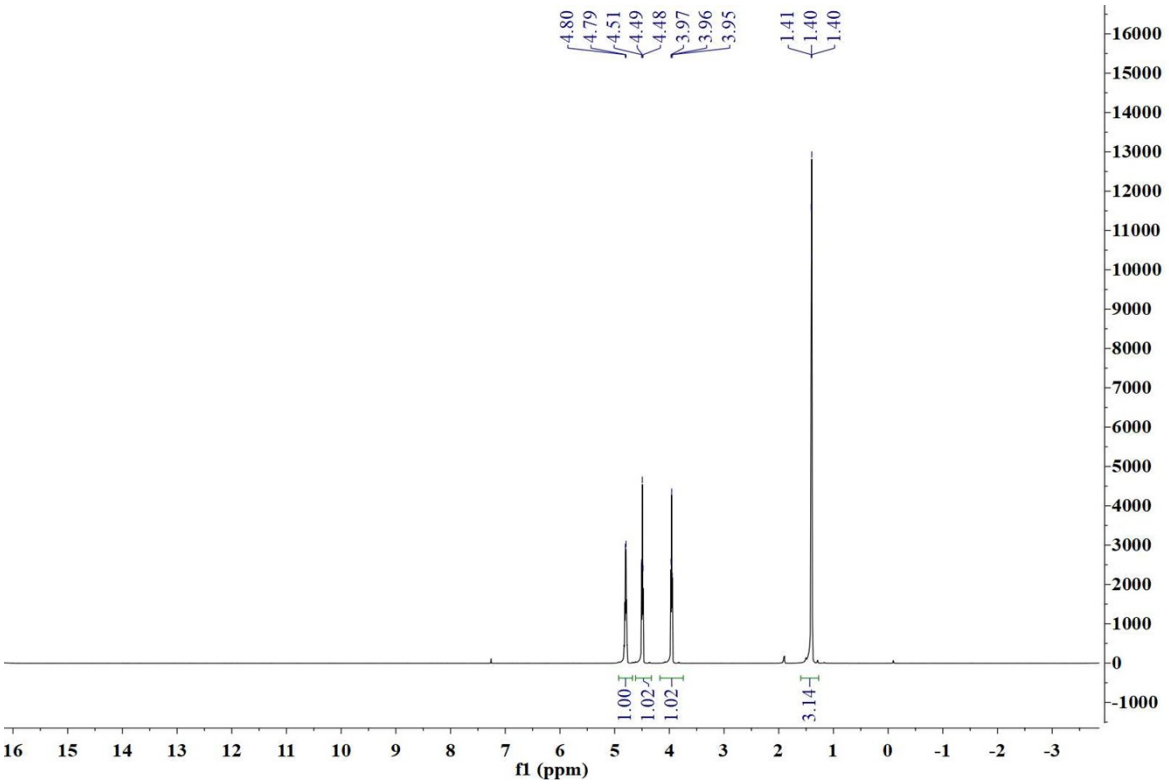
4.80
4.79
4.51
4.49
4.48
3.97
3.96
3.95
1.41
1.40
1.40
1.00
1.02
1.02
3.14
f1 (ppm)

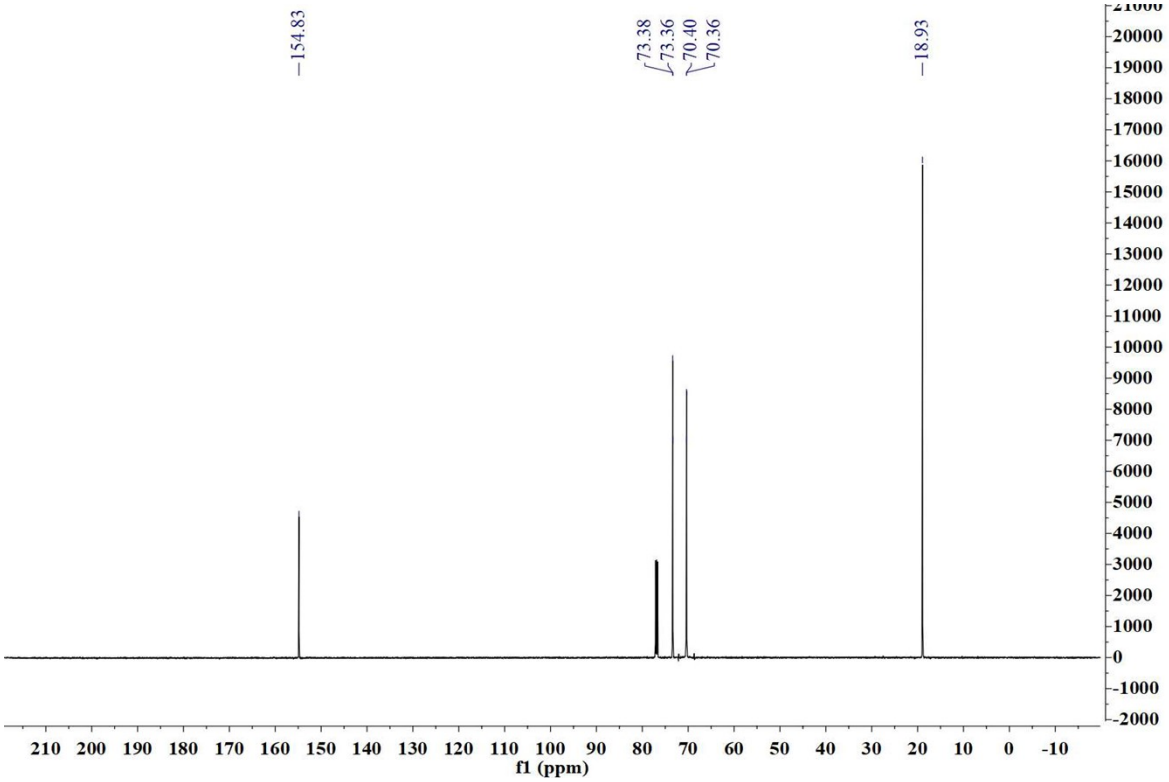
154.83
73.38
73.36
70.40
70.36
18.93
f1 (ppm)

1e

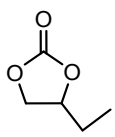

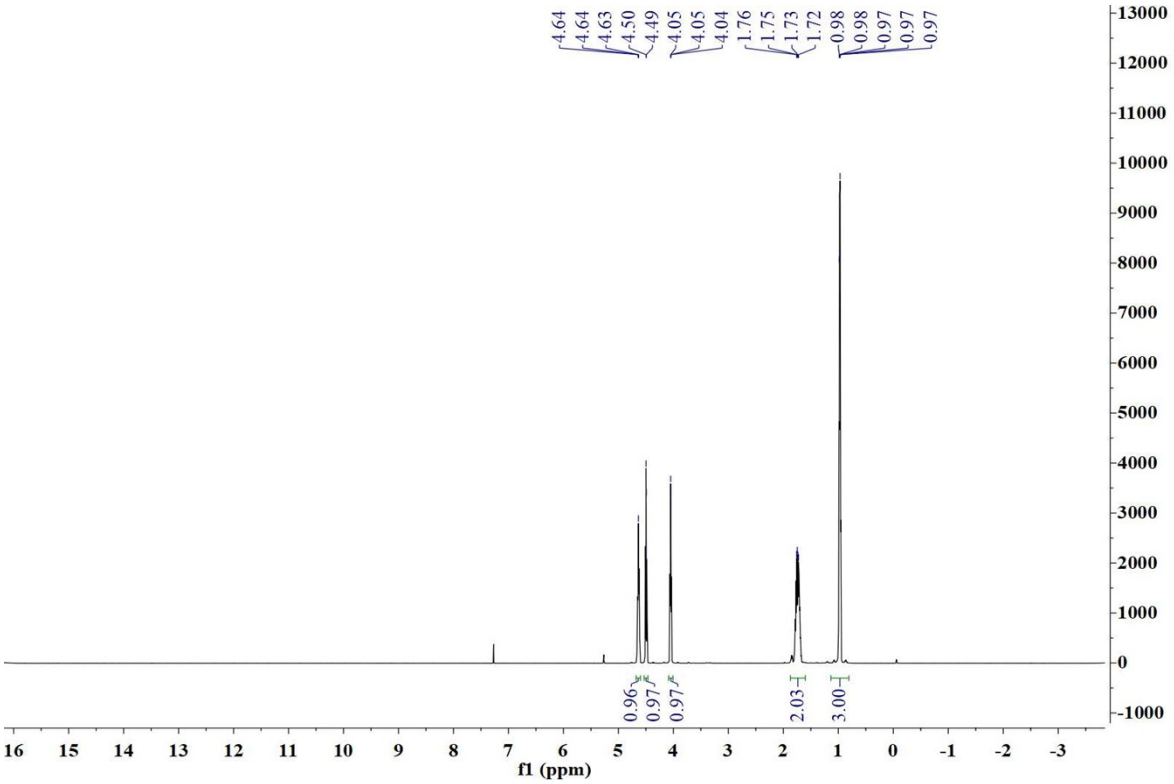
4.64
4.64
4.63
4.50
4.49
4.05
4.05
4.04
1.76
1.75
1.73
1.72
0.98
0.98
0.97
0.97
0.97
0.96
0.97
0.97
2.03
3.00
f1 (ppm)

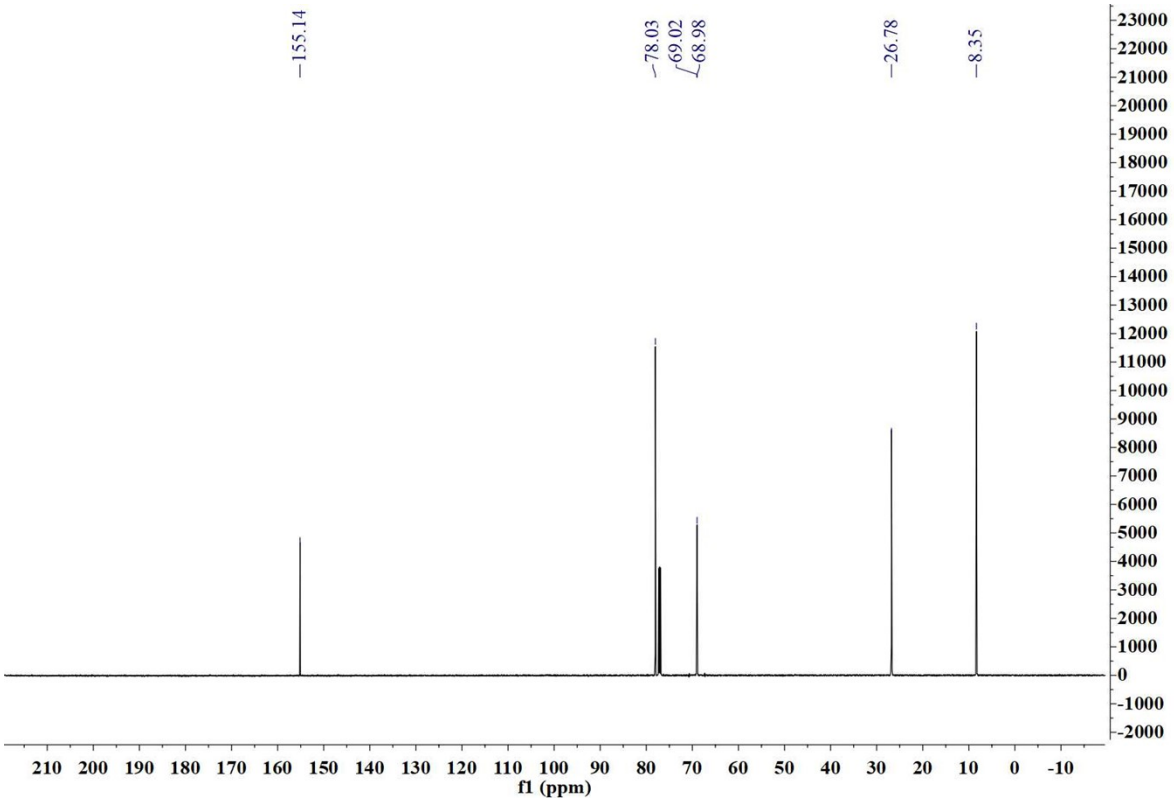
155.14
78.03
69.02
68.98
26.78
8.35
f1 (ppm)

1f

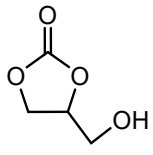
O
O
O
OH

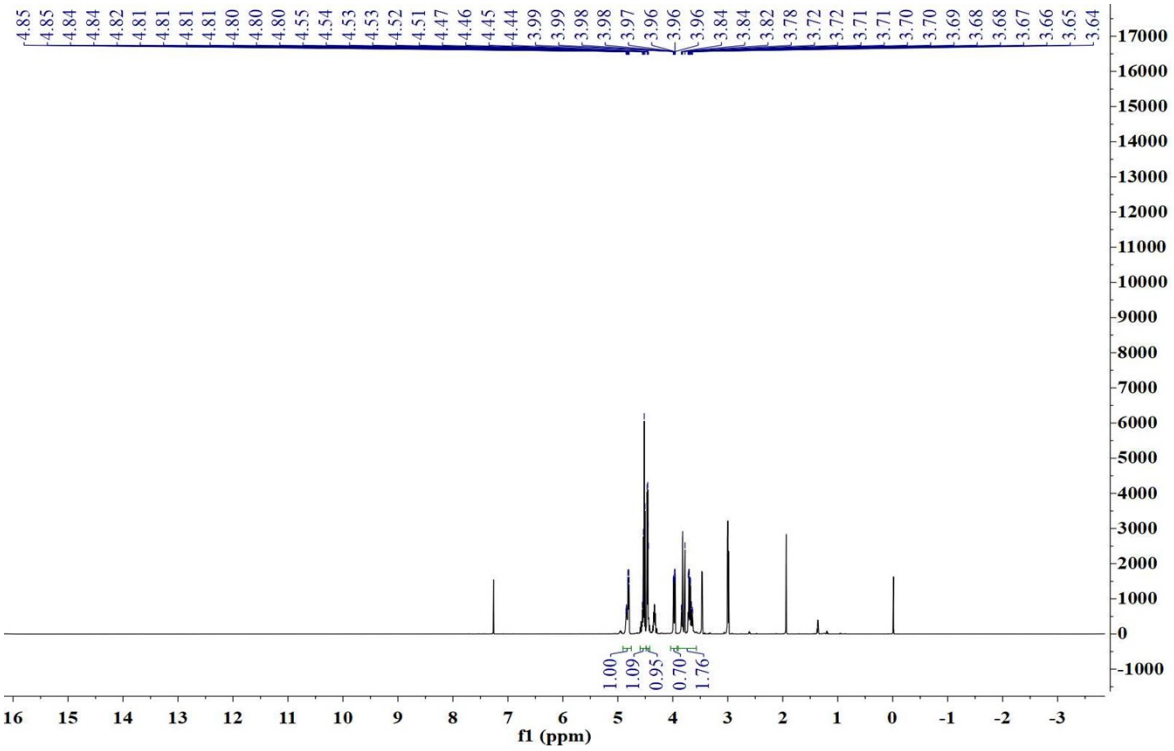
4.85 4.85 4.84 4.84 4.82 4.81 4.81 4.81 4.81 4.80 4.80 4.80 4.55 4.54 4.53 4.53 4.52 4.51 4.47 4.46 4.45 4.44 3.99 3.99 3.98 3.98 3.97 3.96 3.96 3.96 3.84 3.84 3.82 3.78 3.72 3.72 3.71 3.71 3.70 3.70 3.69 3.68 3.68 3.67 3.66 3.65 3.64
1.00 1.09 0.95 0.70 1.76
f1 (ppm)

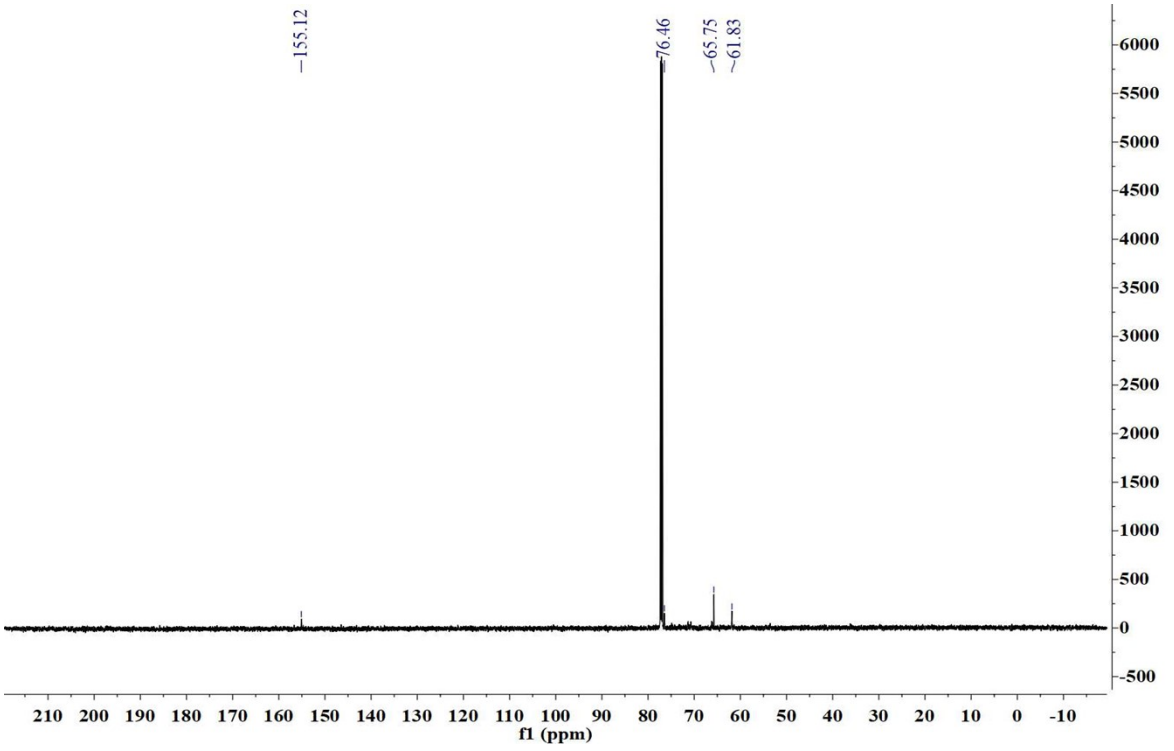
155.12
76.46
65.75
61.83
f1 (ppm)

1g

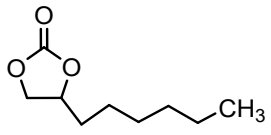
O
O
O
CH3

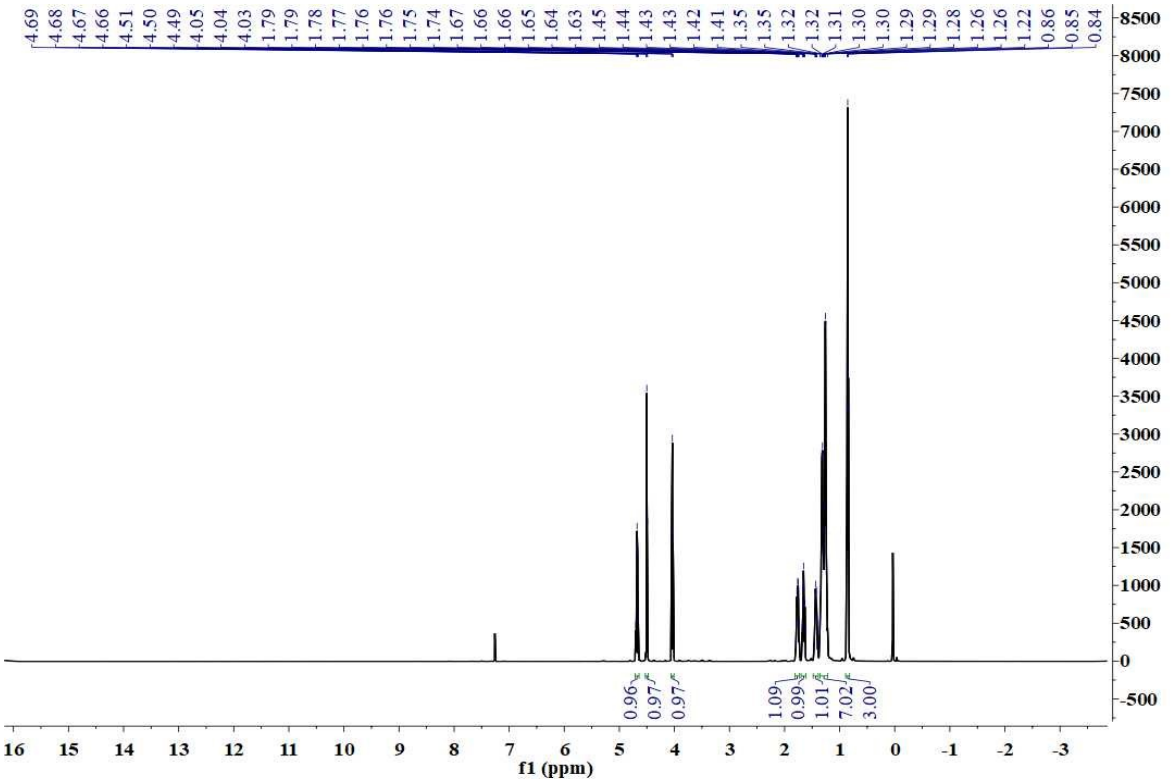
4.69 4.68 4.67 4.66 4.51 4.50 4.49 4.05 4.04 4.03 1.79 1.79 1.78 1.77 1.76 1.76 1.75 1.74 1.67 1.66 1.66 1.65 1.64 1.63 1.45 1.44 1.43 1.43 1.42 1.41 1.35 1.35 1.32 1.32 1.31 1.30 1.30 1.29 1.29 1.28 1.26 1.26 1.22 0.86 0.85 0.84
0.96 0.97 0.97 1.09 0.99 1.01 7.02 3.00
f1 (ppm)

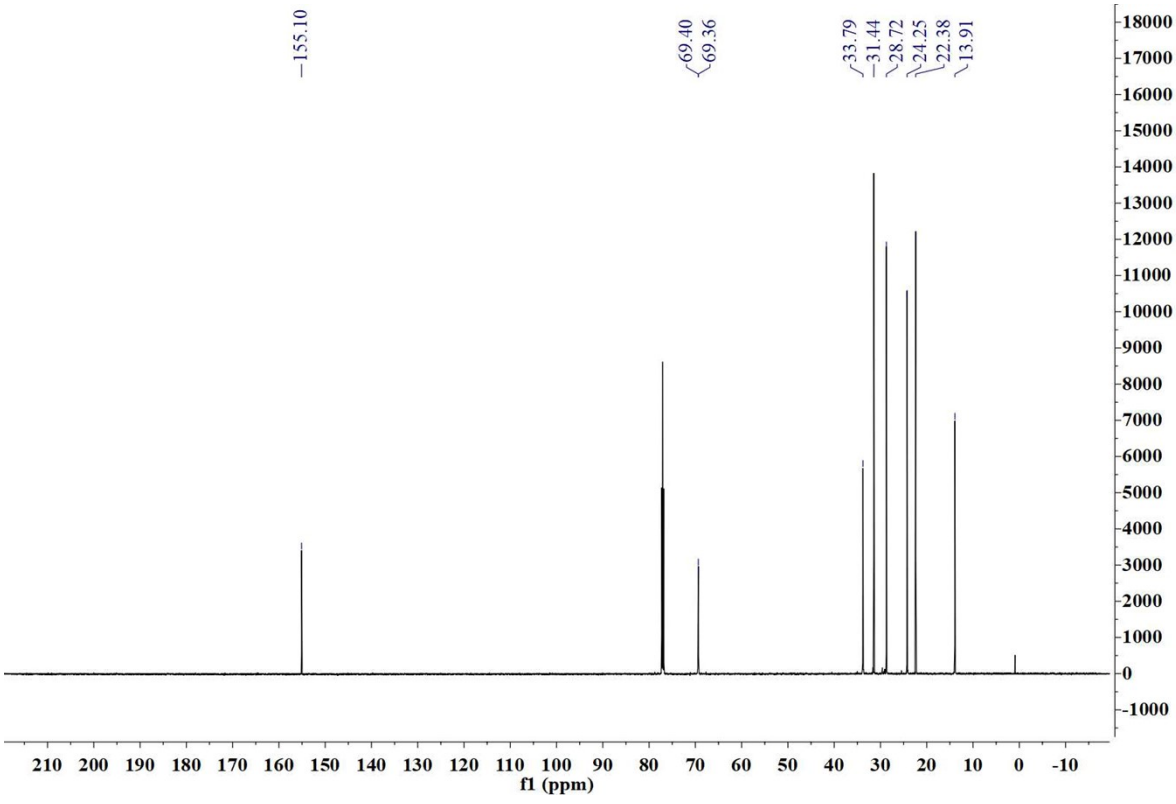
155.10
69.40 69.36
33.79 31.44 28.72 24.25 22.38 13.91
f1 (ppm)

1h

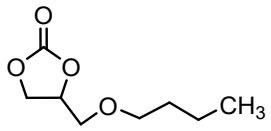
O
O
O
O
CH3

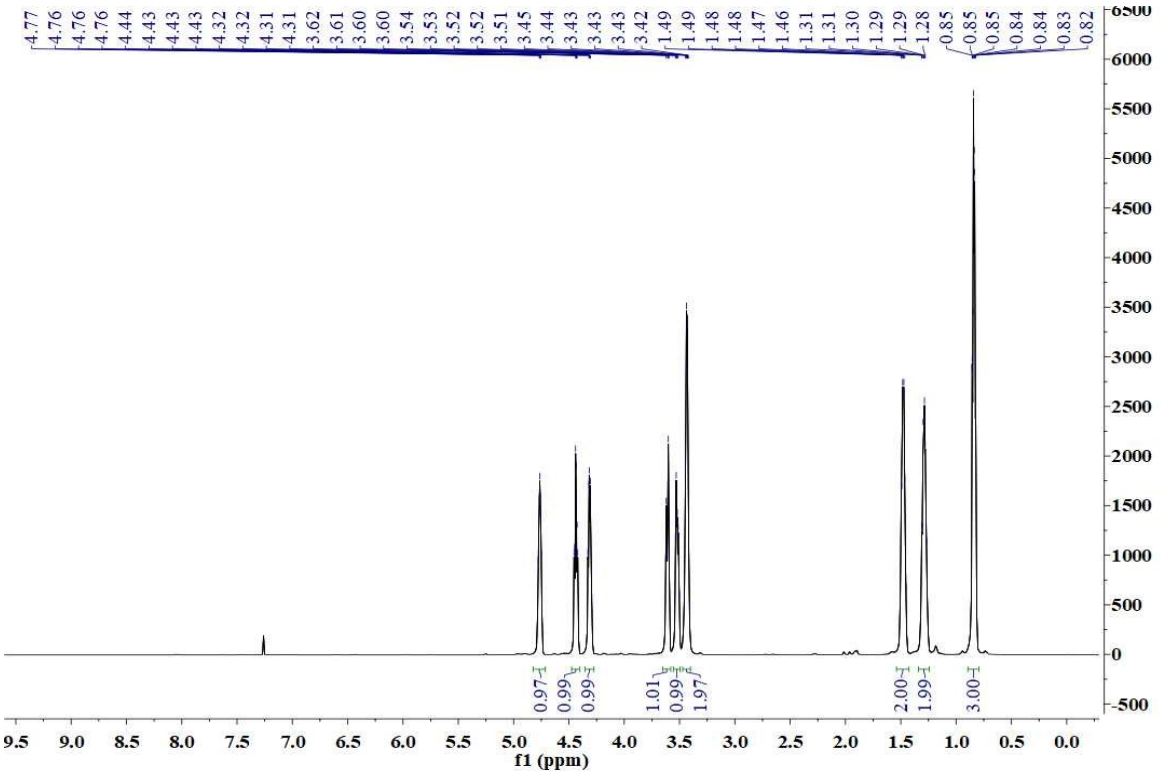
4.77
4.76
4.76
4.76
4.44
4.43
4.43
4.43
4.32
4.31
4.31
3.62
3.61
3.60
3.60
3.54
3.53
3.52
3.52
3.51
3.45
3.44
3.43
3.43
3.43
3.42
1.49
1.49
1.48
1.48
1.47
1.46
1.31
1.31
1.30
1.29
1.29
1.28
0.85
0.85
0.85
0.84
0.84
0.83
0.82
0.97
0.99
0.99
1.01
0.99
1.97
2.00
1.99
3.00
f1 (ppm)

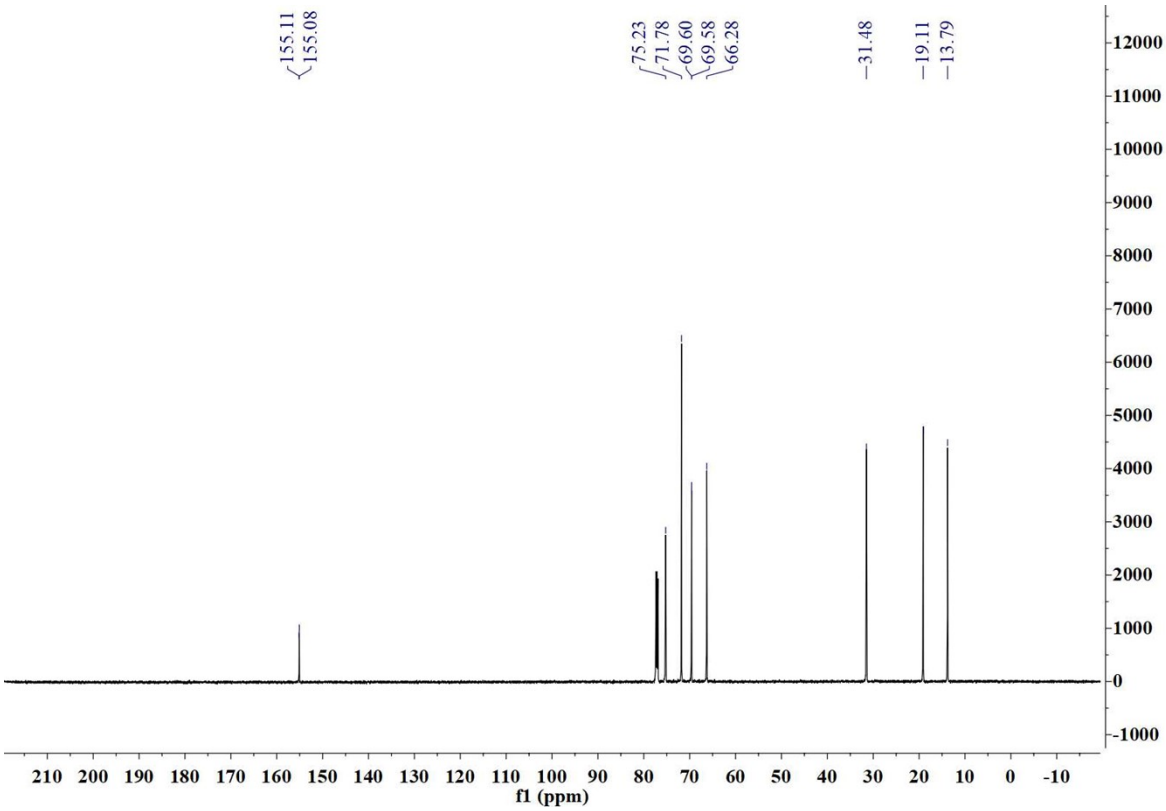
155.11
155.08
75.23
71.78
69.60
69.58
66.28
31.48
19.11
13.79
f1 (ppm)

1i

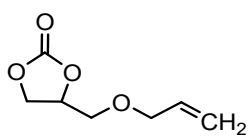
O
O
O
O
CH2

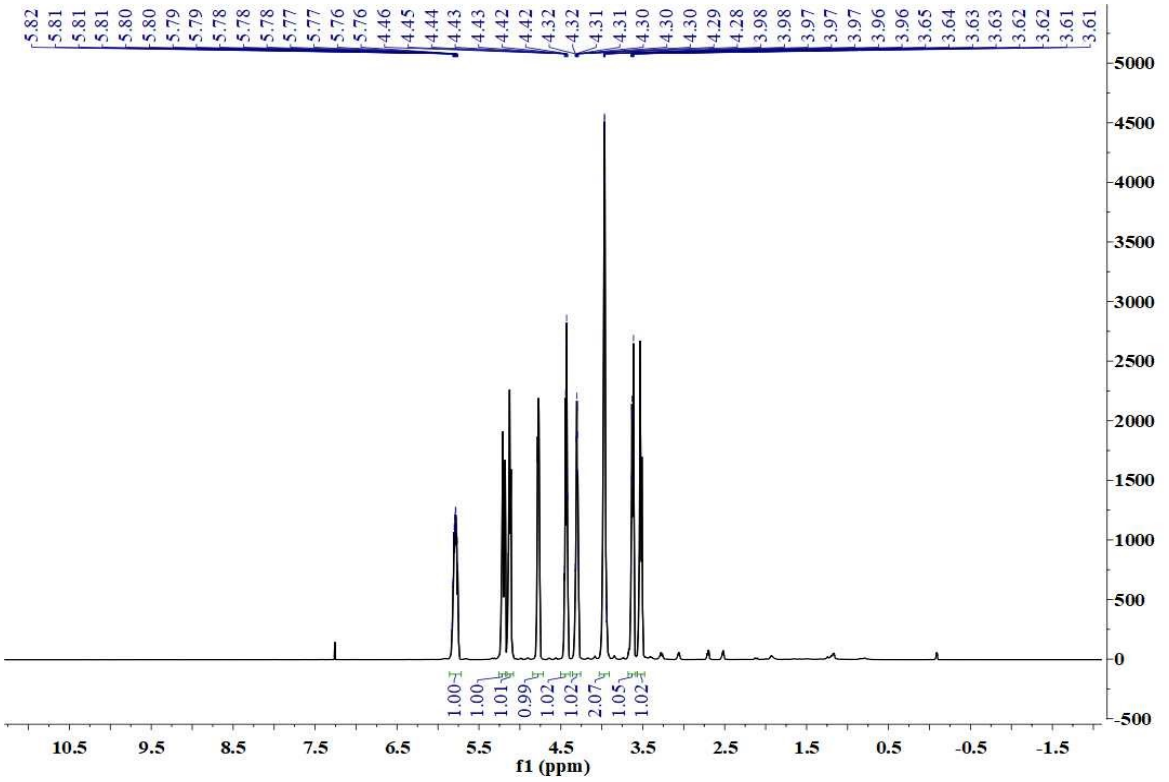
5.82 5.81 5.81 5.81 5.80 5.80 5.79 5.79 5.78 5.78 5.78 5.77 5.77 5.76 5.76 4.46 4.45 4.44 4.43 4.43 4.42 4.42 4.32 4.32 4.31 4.31 4.30 4.30 4.29 4.28 3.98 3.98 3.97 3.97 3.96 3.96 3.65 3.64 3.63 3.63 3.62 3.62 3.61 3.61
1.00 1.00 1.01 0.99 1.02 1.02 2.07 1.05 1.02
f1 (ppm)

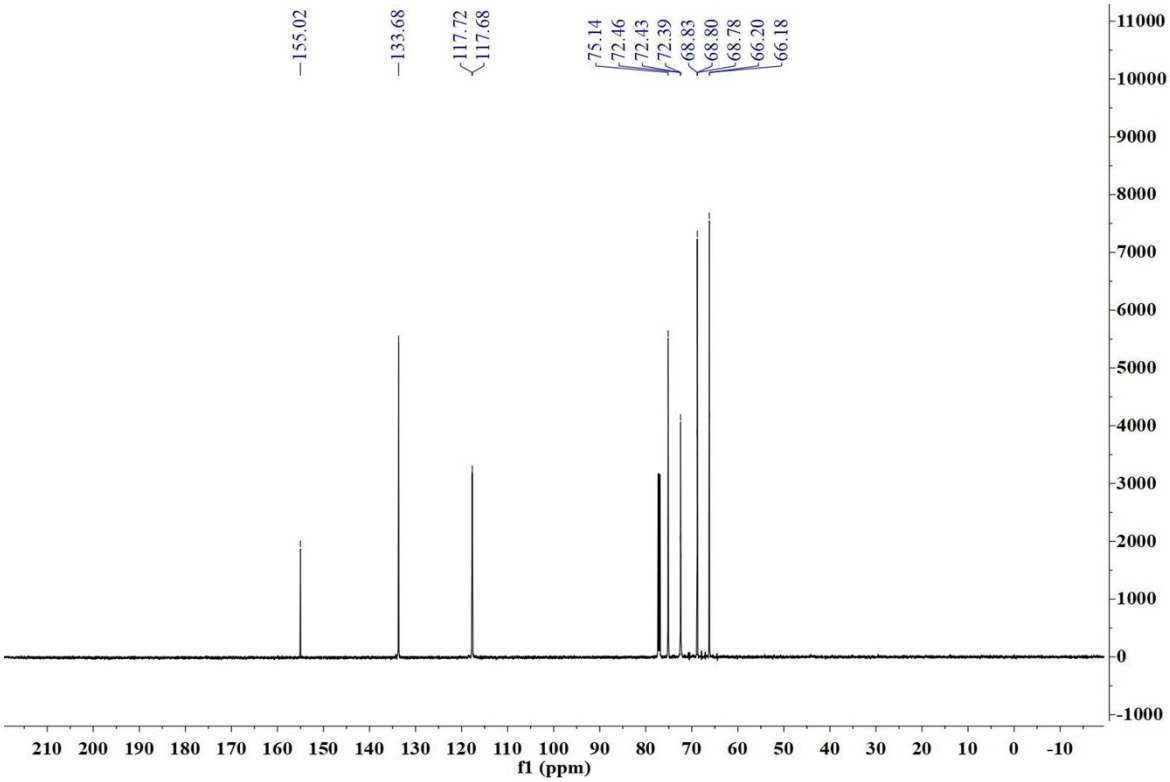
155.02 133.68 117.72 117.68 75.14 72.46 72.43 72.39 68.83 68.80 68.78 66.20 66.18
f1 (ppm)

1j

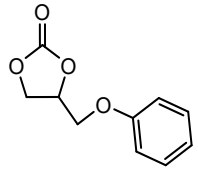

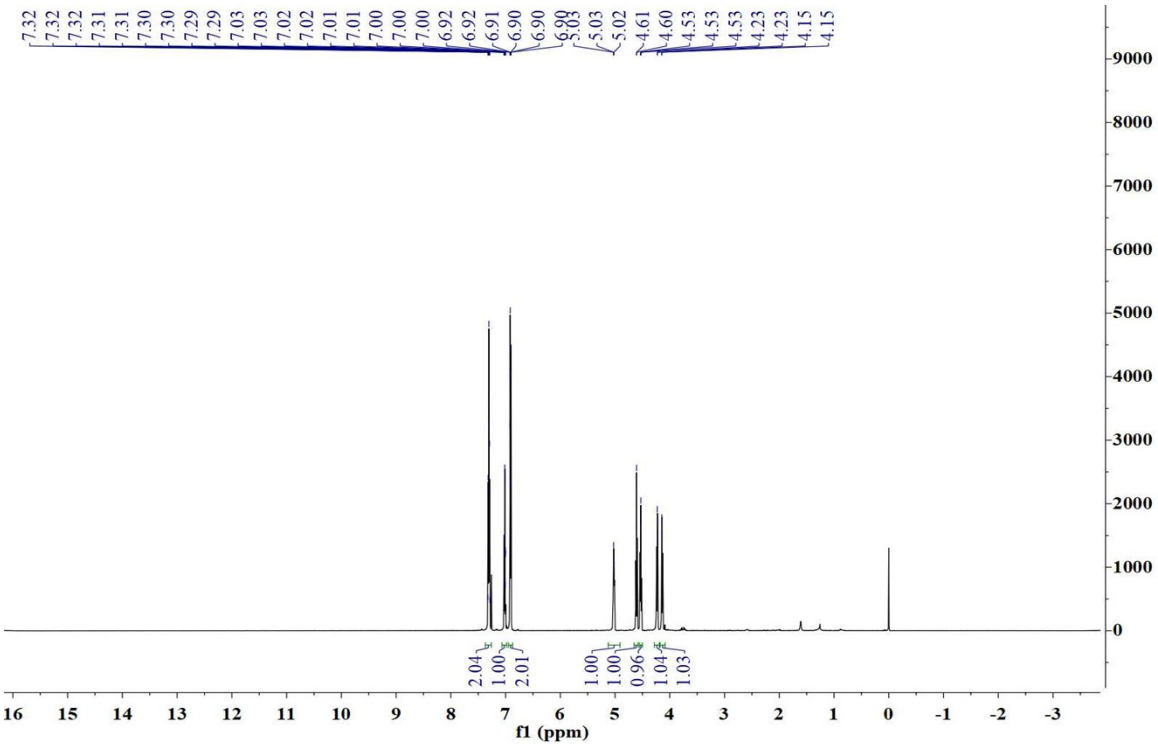
7.32
7.32
7.32
7.31
7.31
7.30
7.30
7.29
7.29
7.03
7.03
7.02
7.02
7.01
7.01
7.00
7.00
7.00
6.92
6.92
6.91
6.90
6.90
6.90
5.03
5.03
5.02
4.61
4.60
4.53
4.53
4.53
4.23
4.23
4.15
4.15
2.04
1.00
2.01
1.00
1.00
0.96
1.04
1.03
f1 (ppm)

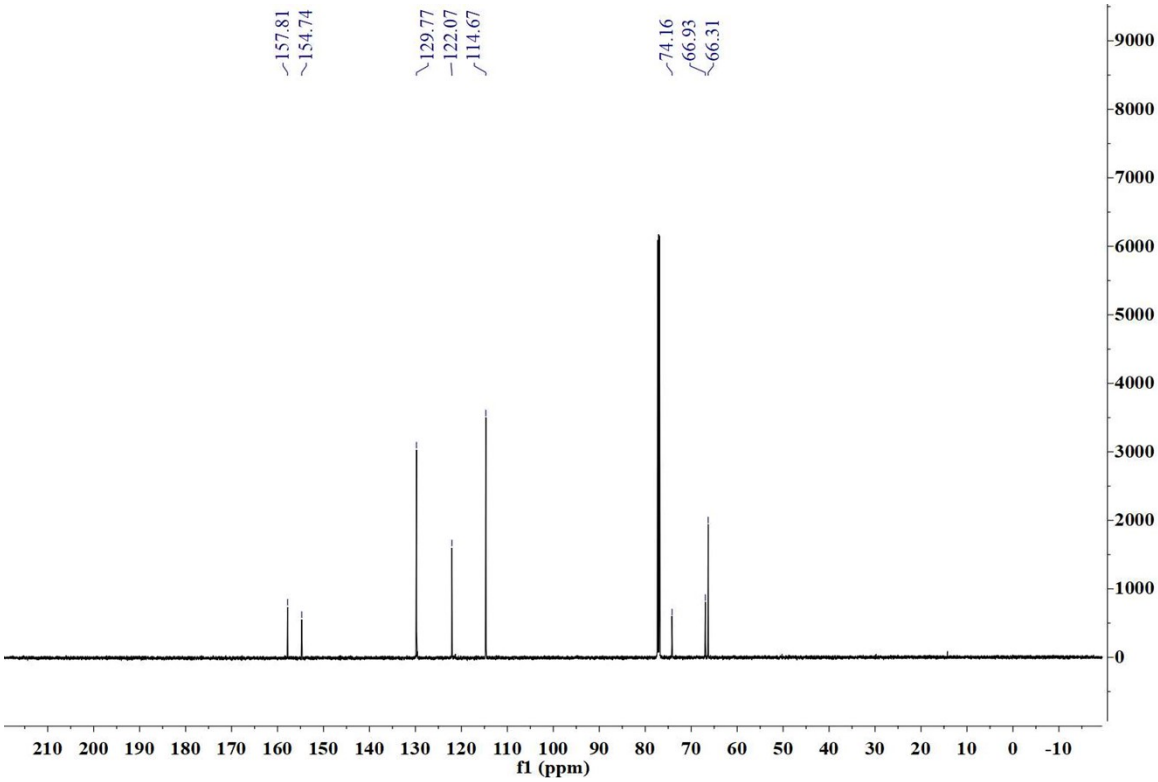
157.81
154.74
129.77
122.07
114.67
74.16
66.93
66.31
f1 (ppm)

1k

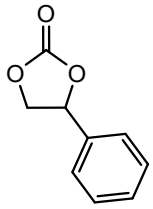

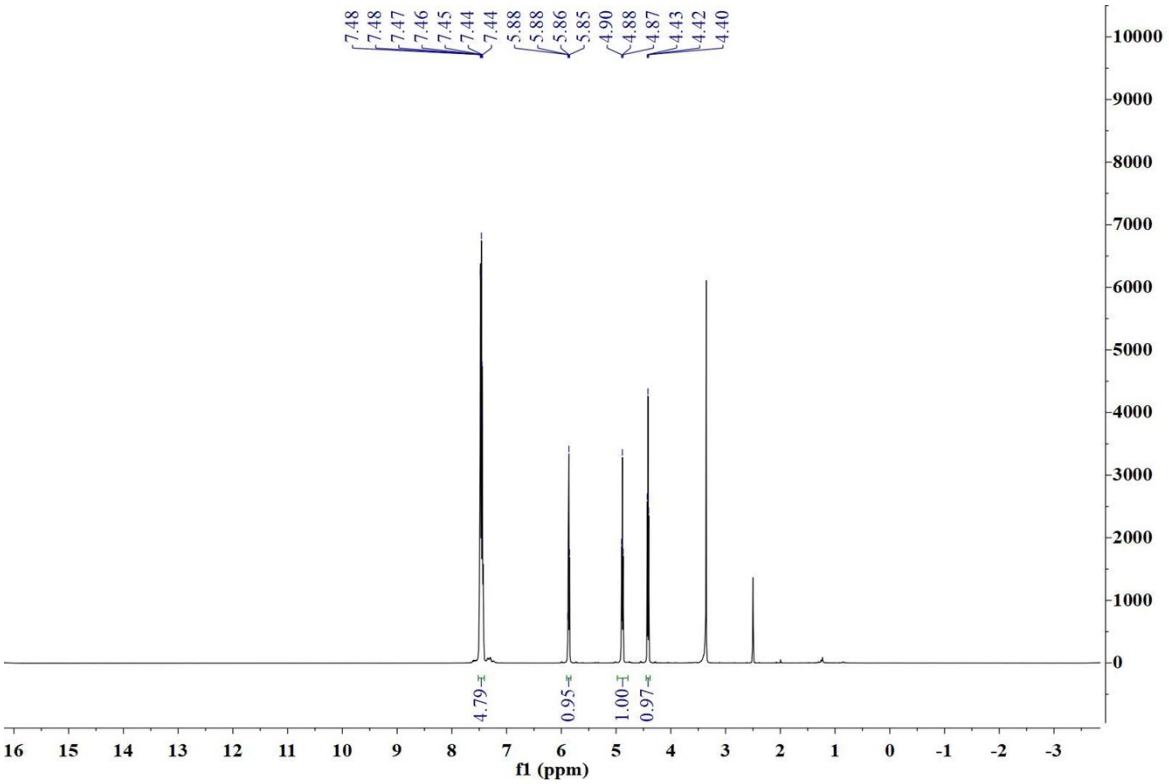
7.48
7.48
7.47
7.46
7.45
7.44
7.44
5.88
5.88
5.86
5.85
4.90
4.88
4.87
4.43
4.42
4.40
4.79
0.95
1.00
0.97
f1 (ppm)

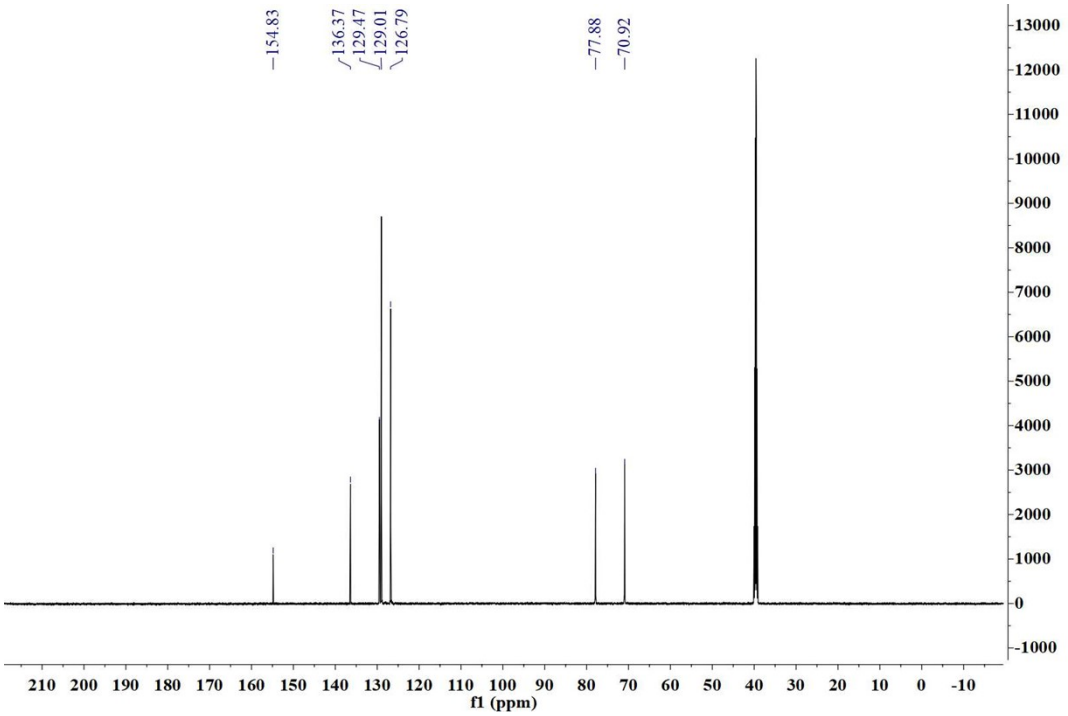
154.83
136.37
129.47
129.01
126.79
77.88
70.92
f1 (ppm)

1l

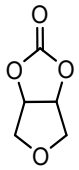

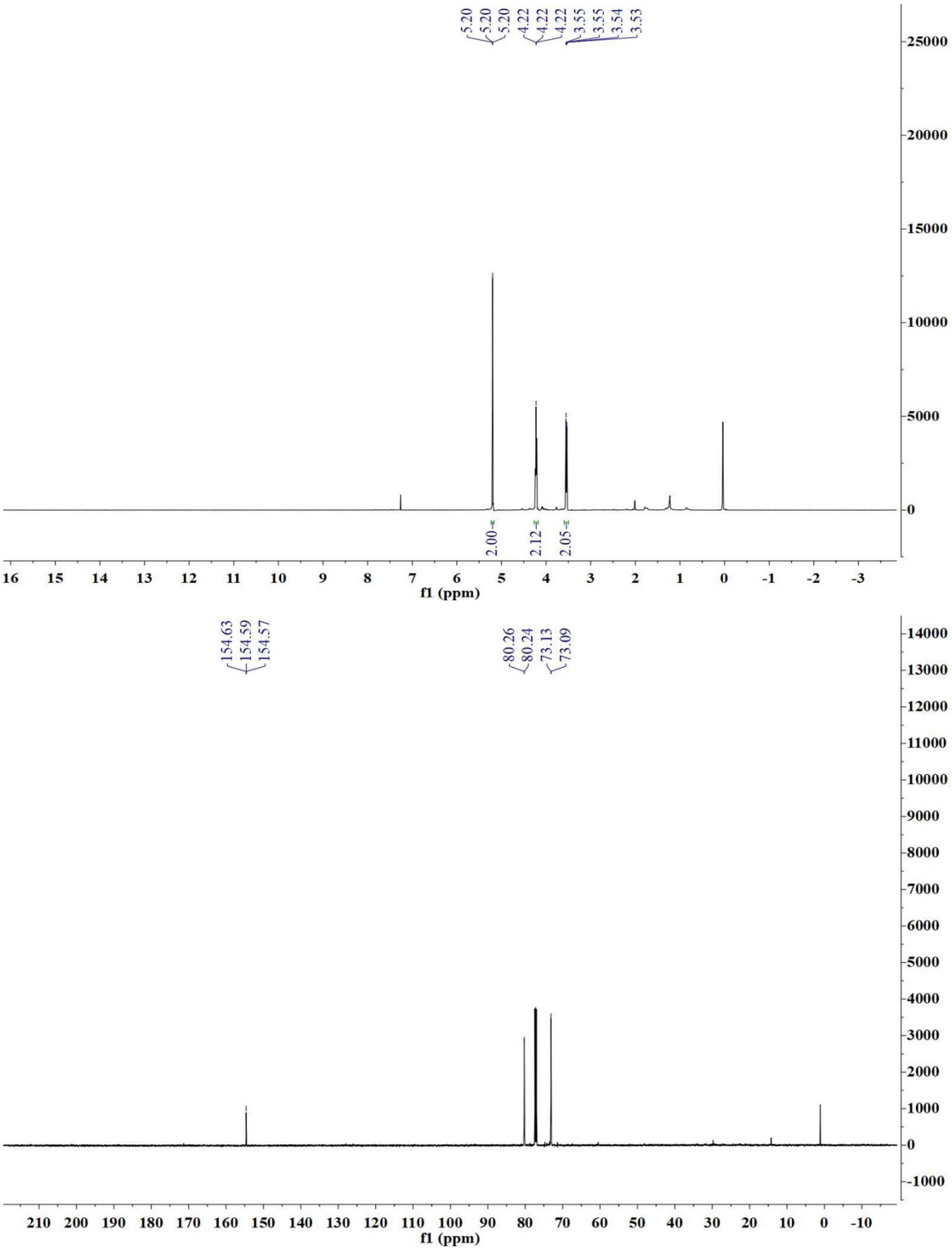

References

[1] A.D. Becke, Density-functional thermochemistry. III. The role of exact exchange, J. Chem. Phys. 98 (1993) 5648−5652.

[2] J. P. Perdew, K. Burke, Y. Wang, Generalized gradient approximation for the exchange correlation hole of a many-electron system, Phys. Rev. B. 54 (1996)

16533−16539.

[3] P.M.W. Gill, B.G. Johnson, J.A. Pople, M.J. Frisch, The performance of the Becke-Lee-Yang-Parr (B-LYP) density functional theory with various basis sets, Chem. Phys. Lett. 197 (1992) 499−505.

[4] S. Miertuš, E. Scrocco, J. Tomasi, Electrostatic interaction of a solute with a continuum. A direct utilizaion of AB initio molecular potentials for the prevision of solvent effects, Chem. Phys. 55 (1981) 117−129.

[5] S. Miertuš, J. Tomasi, Approximate evaluations of the electrostatic free energy and internal energy changes in solution processes, Chem. Phys. 65 (1982) 239−245.